Journal of Human Evolution 180 (2023) 103385

Contents lists available at ScienceDirect

Journal of Human Evolution

journal homepage: www.elsevier.com/locate/jhevol

Pliocene hominins from East Turkana were associated with mesic environments in a semiarid basin

Amelia Villaseñor [a, *], Kevin T. Uno [b], Rahab N. Kinyanjui [c, d, e], Anna K. Behrensmeyer [f], René Bobe [g, h], Eldert L. Advokaat [i], Marion Bamford [j], Susana C. Carvalho [g, h, k], Ashley S. Hammond [l, m], Dan V. Palcu [n, o], Mark J. Sier [p, q, i], Carol V. Ward [r], David R. Braun [s]

[a] Department of Anthropology, The University of Arkansas, 330 Old Main, Fayetteville, AR, 72701, USA
[b] Lamont-Doherty Earth Observatory of Columbia University, Division of Biology and Paleo Environment, Palisades, NY, 10964, USA
[c] Department of Earth Sciences, National Museums of Kenya, Nairobi, 40658-00100, Kenya
[d] Department of Archaeology, Max Planck Institute of Geoanthropology, 07745, Jena, Germany
[e] Human Origins Program, National Museum of Natural History, Smithsonian Institution, MRC 121, Washington, DC, 20013, USA
[f] Department of Paleobiology, National Museum of Natural History, Smithsonian Institution, MRC 121, Washington, DC, 20013, USA
[g] Primate Models for Behavioural Evolution Lab, Institute of Human Sciences, University of Oxford, 64 Banbury Road, Oxford, OX2 6PN, UK
[h] Gorongosa National Park, Sofala, Mozambique
[i] Department of Earth Sciences, Utrecht University, Princetonlaan 8A, 3584 CB Utrecht, the Netherlands
[j] Evolutionary Studies Institute and School of Geosciences, University of the Witwatersrand, P Bag 3, WITS, 2050, South Africa
[k] Interdisciplinary Center for Archaeology and Evolution of Human Behaviour (ICArEHB), Universidade do Algarve, 8005-139, Faro, Portugal
[l] Division of Anthropology, American Museum of Natural History (AMNH), New York, NY, 10024, USA
[m] New York Consortium in Evolutionary Primatology at AMNH, New York, NY, 10024, USA
[n] Oceanographic Institute of the University of São Paulo, Brazil
[o] Paleomagnetic Laboratory 'Fort Hoofddijk', Utrecht University, Budapestlaan 17, 3584 CD, Utrecht, the Netherlands
[p] Centro Nacional de Investigación Sobre la Evolución Humana (CENIEH), Paseo Sierra de Atapuerca 3, 09002, Burgos, Spain
[q] Department of Earth Sciences, University of Oxford, South Parks Road, OX1 3AN, Oxford, UK
[r] Department of Pathology and Anatomical Sciences, University of Missouri, Columbia, MO, USA
[s] Center for the Advanced Study of Human Paleobiology, Anthropology Department, George Washington University, Washington, DC, USA

ARTICLE INFO

Article history:
Received 3 June 2022
Accepted 19 April 2023

Keywords:
Middle Pliocene hominin paleoecology
Multiproxy
Stable isotope ecology
Australopithecus afarensis
Kenyanthropus platyops
Koobi Fora

ABSTRACT

During the middle Pliocene (~3.8–3.2 Ma), both *Australopithecus afarensis* and *Kenyanthropus platyops* are known from the Turkana Basin, but between 3.60 and 3.44 Ma, most hominin fossils are found on the west side of Lake Turkana. Here, we describe a new hominin locality (ET03-166/168, Area 129) from the east side of the lake, in the Lokochot Member of the Koobi Fora Formation (3.60–3.44 Ma). To reconstruct the paleoecology of the locality and its surroundings, we combine information from sedimentology, the relative abundance of associated mammalian fauna, phytoliths, and stable isotopes from plant wax biomarkers, pedogenic carbonates, and fossil tooth enamel. The combined evidence provides a detailed view of the local paleoenvironment occupied by these Pliocene hominins, where a biodiverse community of primates, including hominins, and other mammals inhabited humid, grassy woodlands in a fluvial floodplain setting. Between <3.596 and 3.44 Ma, increases in woody vegetation were, at times, associated with increases in arid-adapted grasses. This suggests that Pliocene vegetation included woody species that were resilient to periods of prolonged aridity, resembling vegetation structure in the Turkana Basin today, where arid-adapted woody plants are a significant component of the ecosystem. Pedogenic carbonates indicate more woody vegetation than other vegetation proxies, possibly due to differences in temporospatial scale and ecological biases in preservation that should be accounted for in future studies. These new hominin fossils and associated multiproxy paleoenvironmental indicators from a single locale through time suggest that early hominin species occupied a wide range of habitats, possibly including wetlands within semiarid landscapes. Local-scale paleoecological evidence from East Turkana supports regional evidence that middle Pliocene eastern Africa may have experienced large-scale, climate-driven periods of aridity. This information extends our understanding of hominin environments beyond the limits of simple wooded, grassy, or mosaic environmental descriptions.

* Corresponding author.
E-mail address: avillase@uark.edu (A. Villaseñor).

https://doi.org/10.1016/j.jhevol.2023.103385
0047-2484/

1. Introduction

Middle Pliocene hominins (3.8–3.2 Ma) were taxonomically diverse and geographically widespread within Africa (e.g., Behrensmeyer and Reed, 2013; Haile-Selassie et al., 2015; Spoor et al., 2016). Despite the increase in our knowledge of Pliocene hominin diversity, the environmental constraints associated with the ranges of these hominins are best known from only a handful of localities. Abundant fossils and detailed paleoecological work from sites such as Hadar, Ethiopia, West Turkana, Kenya, and Laetoli, Tanzania, provide the primary basis of our ecological and evolutionary knowledge of Pliocene hominin taxa (e.g., Kimbel et al., 1994; Leakey et al., 2001; Bobe et al., 2002; Drapeau et al., 2005; Campisano and Feibel, 2008; Reed, 2008; Kimbel and Delezene, 2009; Harrison, 2011a,b; Ward et al., 2020). Both *Kenyanthropus platyops* and *Australopithecus afarensis* are argued to have been present in middle Pliocene Kenya and had similar adaptive strategies, including potential tool use and the incorporation of C_4 resources into their diets (Kimbel, 1988; Leakey et al., 2001; Ungar et al., 2010; Cerling et al., 2013; Delezene et al., 2013; Harmand et al., 2015; Mbua et al., 2016; Wynn et al., 2020).

Regional paleoecological analyses of the middle Pliocene Horn of Africa revealed periods of prolonged aridity resulting in an abundance of arid-adapted vegetation such as Amaranthaceae and Chloridoideae (Bonnefille, 2010; Liddy et al., 2016). However, the rift valley is tectonically active, creating topographical complexity that contributes to a variety of microclimates. Thus, while the region became drier, some areas likely remained relatively mesic. As documented in modern rift valley ecosystems (e.g., Lake Manyara), vegetation on either side of a lake can be drastically different due to the presence of freshwater springs and differences in topography (Barboni et al., 2019). These differences are particularly stark in semiarid environments prevalent throughout the rift today and in the past (Bobe, 2006). Thus, detailed, local-scale paleoenvironmental reconstructions are needed to develop a nuanced understanding of the hominin niche.

Fossils are not equally represented across time and space due to taphonomic factors, such as burial environments and sedimentation rates, which limit the reconstruction of hominin ecology. Pliocene fossils are more abundant in the Awash Valley of the Afar Basin in Ethiopia than they are in the Turkana Basin in Kenya (Villaseñor et al., 2020). This has been attributed to lower depositional rates in the Turkana Basin, hence lower probability of burial and preservation of hominin remains (Campisano and Feibel, 2007). Within the Turkana Basin, fewer middle Pliocene hominin fossils are documented from East Turkana than from West Turkana (Villaseñor et al., 2020). Until now, very few hominin fossils were known from East Turkana's Lokochot member (3.60–3.44) (Leakey, 1976), though an extensive collection of hominins derives from contemporaneous sediments at Lomekwi on the west side of Lake Turkana (Leakey et al., 2001; Skinner et al., 2020). Additional paleontological records of fossils and multiproxy comparisons from the lesser-known regions, such as East Turkana, could provide key insights into the environmental tolerance of middle Pliocene hominin species and additional information about their ecological niches.

Here, we present a multiproxy analysis of the paleoenvironment of the Lokochot Member of the Koobi Fora Formation (Fig. 1), where the recovery of new hominin specimens can be placed within a discrete geochronological and paleoecological context. The hominin specimens are from a new site in Area 129, ET03-166/168, discovered during a systematic stratigraphic survey led by authors A.K.B. and R.B. in 2003. The first hominin fossil at ET03-166/168 was found by Robert Moru. Tom Mukhuyu, Catherine Haradon, and James Murage also participated in the systematic survey in 2003 and recovered mammal fossils associated with the first hominin. Continued paleontological work at the site and in the region has recovered additional hominin and mammal fossils. Both the hominin and associated mammal fossils from ET03-166/168 are eroding out of a floodplain paleosol at the base of a sedimentary sequence that includes fluvial sands, silts, and clays (NL129-17; Fig. 2). Contemporaneous mammalian community ecology, phytoliths, and stable isotope data from pedogenic carbonates, plant wax biomarkers, and large mammal enamel from this sequence represent an opportunity to explore detailed local- and regional-scale ecological records at a single paleontological locality. We also discuss the relationships and biases of the multiproxy evidence. Taken together, these data provide the basis for a broader understanding of the middle Pliocene hominin niche.

1.1. Multiproxy paleoenvironmental analysis

Multiproxy paleoenvironmental comparisons are complex, in part because each proxy represents different spatial and temporal scales (Davis and Pineda-Munoz, 2016; Du et al., 2019). When considered together, however, ecological reconstructions based on multiple proxies reveal new insights into the hominin environmental niche. For example, multiproxy comparisons can link orbitally driven climate shifts to regional changes in plant communities and innovations in human behavior (e.g., Potts et al., 2018; Lupien et al., 2021). Additionally, paleoenvironmental analyses suggest that middle Pliocene eastern African environments are heterogeneous at the landscape scale (e.g., Reed, 2008; Curran and Haile-Selassie, 2016; Su and Haile-Selassie, 2022). Here, we analyze a variety of paleoenvironmental indicators (e.g., stable isotopes from pedogenic carbonates, enamel, and plant wax biomarkers, along with phytoliths and faunal abundance data) from ET03-166/168 and the surrounding sediments, which are spatially and temporally well constrained by radiometric and paleomagnetic dating. We examine both landscape and local-level interpretations of the environment and place these interpretations within a regional context to gain insight into the ancient biomes affecting hominin evolution. Multiproxy paleontological comparisons provide robust paleoenvironmental interpretations for newly described hominin fossils as well as important examples of limitations when proxies are used in isolation.

1.2. Geochronology and depositional environments of Area 129

The Turkana Basin is a fossiliferous, tectonically active region within the East African Rift Valley System (EARS). Fossils and paleobotanical proxies used in this study derive from Koobi Fora Formation sediments that were deposited on the eastern flank of a large half-graben system within the Turkana Basin (Feibel, 2011; Figs. 1 and 2). The members of the Koobi Fora Formation are designated by underlying tuffs that provide their names (Brown and Feibel, 1986). The hominins and paleoecological information described here derive from the Lokochot Member (Fig. 2). East Turkana is further divided into multiple collection areas that span the eastern portion of modern Lake Turkana (Brown and Feibel, 1991). The new fossil data in this study derive from one of two main areas that comprise the majority of Lokochot member outcrops—Area 129. Although the Lokochot Tuff (3.60 ± 0.05) does not outcrop in Area 129, the stratigraphic sections in this area are capped by the overlying Tulu Bor Tuff, which is dated to 3.44 ± 0.041 Ma (Brown, 1982; Cerling and Brown, 1982; Brown and Mcdougall, 2011; WoldeGabriel et al., 2013).

East Turkana's geological history is characterized primarily by deltaic environments and river systems that constrained the

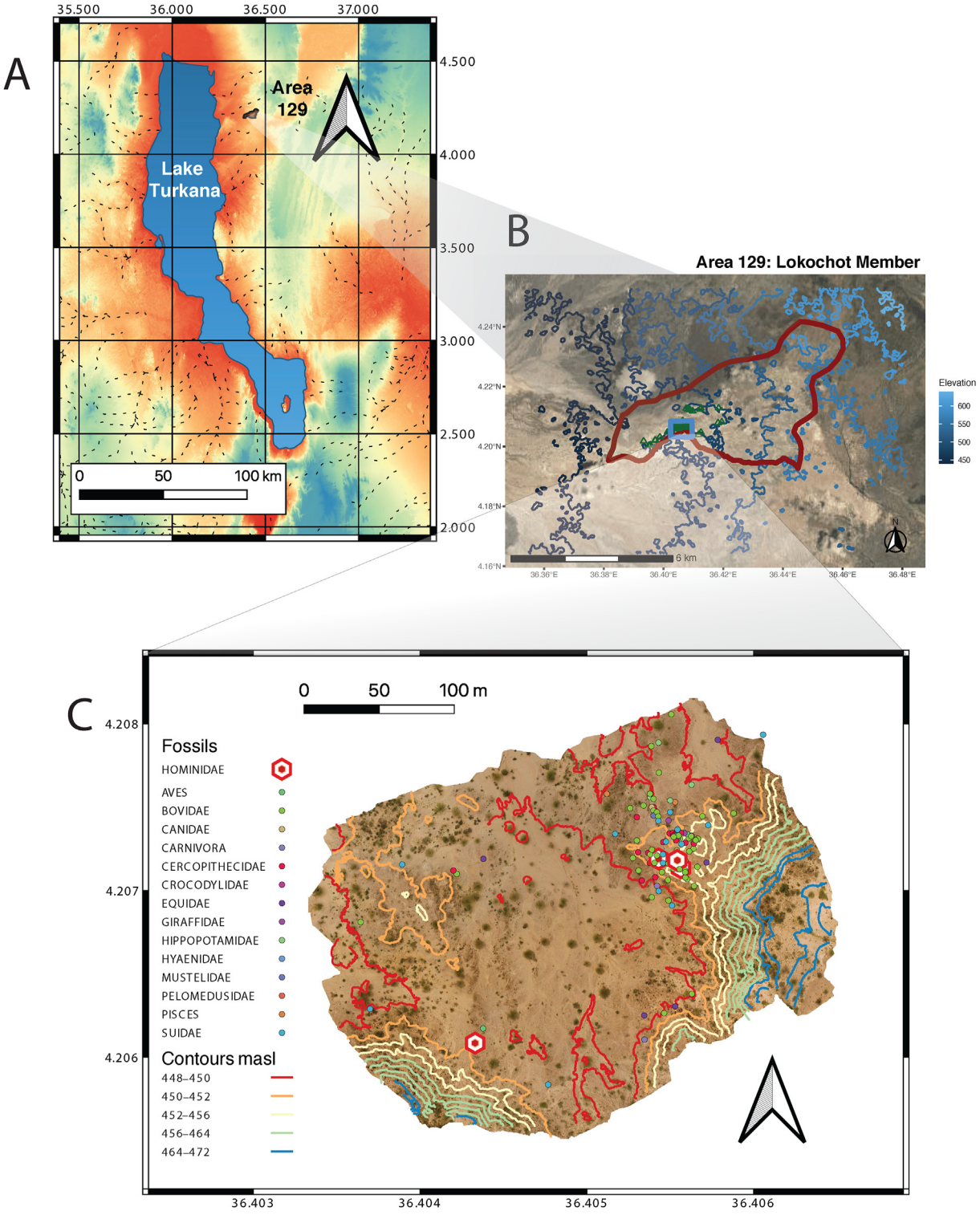

Figure 1. A) Map of the Lake Turkana region with an outline of Area 129 in brown and B) enlarged map of Area 129 with the boundaries outlined in red. Sediments from the Lokochot member are highlighted in green, and the hominin-bearing sediments are outlined in a blue box. C) The primary fossil-bearing area is enlarged. The contour lines represent different elevations at meters above sea level (masl), while the colored circles indicate where different taxa were recovered. (For interpretation of the references to color in this figure legend, the reader is referred to the Web version of this article.)

dominant plant and mammal communities (Harris et al., 1988; Brown and Feibel, 1991; Levin et al., 2011; Villaseñor et al., 2020). The regional vegetation was also affected by shifting climatic and tectonic activity that drove lacustrine or fluvial phases within the Turkana Basin (Bruhn et al., 2011; Levin et al., 2011). The Area 129 ET03-166/168 hominin fossils were recovered from one of the few areas where the Lokochot Member deviates from lacustrine lithofacies that dominate much of this member. Sediments include well-developed paleosols, fine silts and sands with planar and/or cross lamination, and laterally discontinuous channel forms that

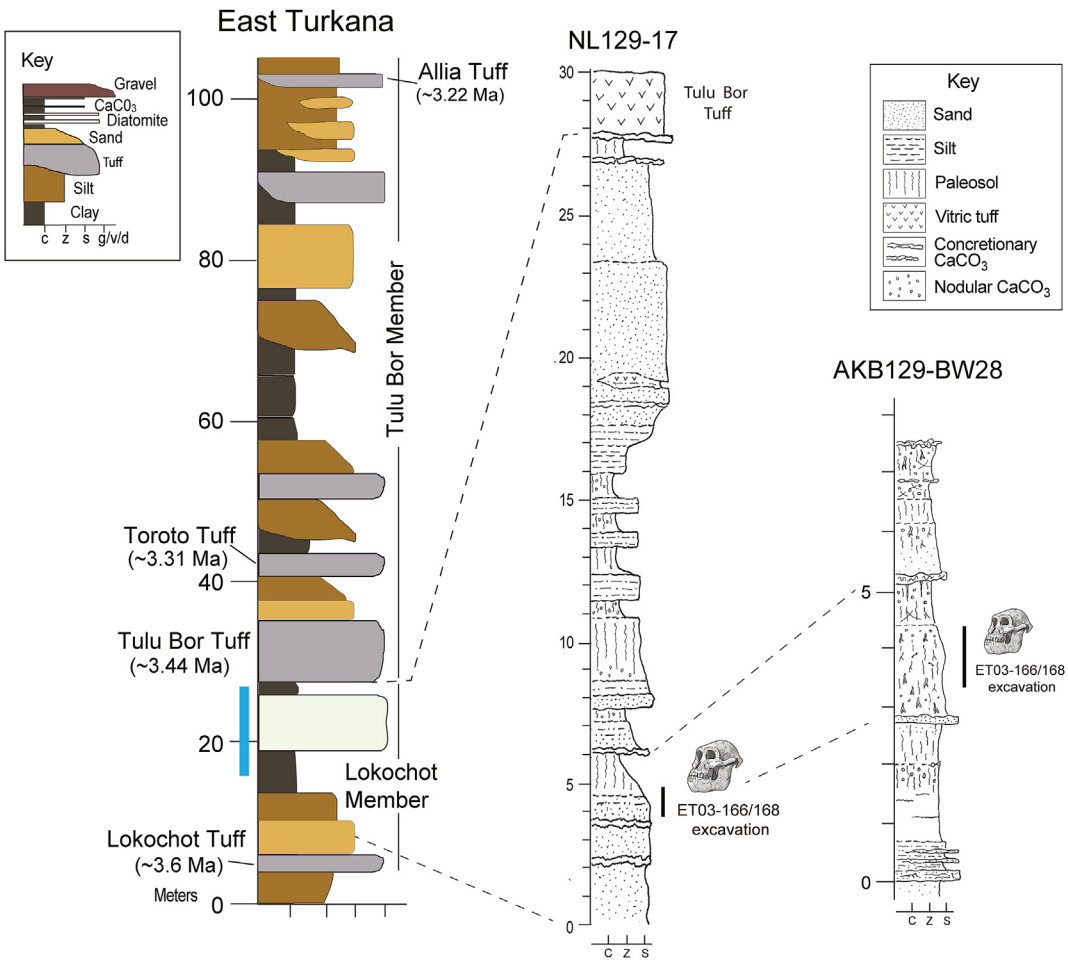

Figure 2. Composite geological sections of East Turkana, Area 129, and microstratigraphic section of the hominin excavation. Each section represents a different resolution of lithology based on the stratigraphic detail available for a particular site. The stratigraphic log for the East Turkana composite is modified from Brown and Feibel (1991). Inferred stratigraphic correlations are indicated by dashed lines. Inferred lacustrine intervals are indicated with a vertical blue line to the left of the East Turkana section; otherwise, the fossiliferous deposits represent fluvial sedimentary environments (channels, levees, crevasse-splays, and floodplains). (For interpretation of the references to color in this figure legend, the reader is referred to the Web version of this article.)

eroded into the underlying mudstones. In the uppermost portion of the section (Fig. 2), a well-developed and laterally extensive paleosol is capped by a thick (>1.5 m) erosion-resistant outcrop of the Tulu Bor Tuff (3.44 Ma), which serves as a marker horizon. A total of seven different pedogenically altered units occur 25 m below this tuff. These paleosols extend to the north and south of the ET03-166/168 locality and were the source for the majority of the pedogenic carbonate and other paleobotanical proxy samples analyzed in this study.

Although the minimum age of the NL129-17 section (Fig. 2) at ET03-166/168 is clearly provided by the Tulu Bor tuff, the maximum age is not well constrained. To provide a more detailed geochronological context, we conducted a paleomagnetic analysis of sediment samples from throughout the geological sequence that begins at the erosional base of the Il Nitirwa River and extends to the top of the Tulu Bor Tuff (Fig. 3). Given the well-known age of this tuff, we expect most of the sediments to fall within the Gauss chron2An (C2An; 2.61–3.596 Ma); specifically, between the Mammoth subchron 2An.2r (3.207–3.33 Ma) and the Gauss to the Gilbert Chron (3.596 Ma; Raffi et al., 2020). The transition from the Gauss to the Gilbert Chron (3.596 Ma) has been documented in the Koobi Fora Formation previously (Hillhouse et al., 1977). Locating this transition within the NL129-17 section would represent a maximum age for these sediments.

1.3. Regional and local faunal diversity and abundance of the Pliocene Turkana Basin

Interbasin and intrabasin studies of fossil assemblages show that the eastern African rift valley supported a diversity of Pliocene mammal communities and habitats (Bobe et al., 2007; Du and Alemseged, 2018; Villaseñor et al., 2020). Comparisons of large mammal fossils indicate that East Turkana had higher species diversity than West Turkana or the Lower Omo Valley during the Pliocene (3.5–3.0 Ma), which may be due to high habitat heterogeneity in East Turkana (Du and Alemseged, 2018). High specimen numbers of bovid taxa associated with mesic habitats also suggest that East Turkana supported extensive floodplains during the middle Pliocene (3.6–3.22 Ma). On the west side of the lake, the fossil bovid community from middle Pliocene West Turkana likely represents drier habitats than in East Turkana (Bobe et al., 2007; Villaseñor et al., 2020). Here, we examine large mammal abundance between 3.60 and 3.44 Ma using fossil databases and systematic surveys of Area 129 to explore local to

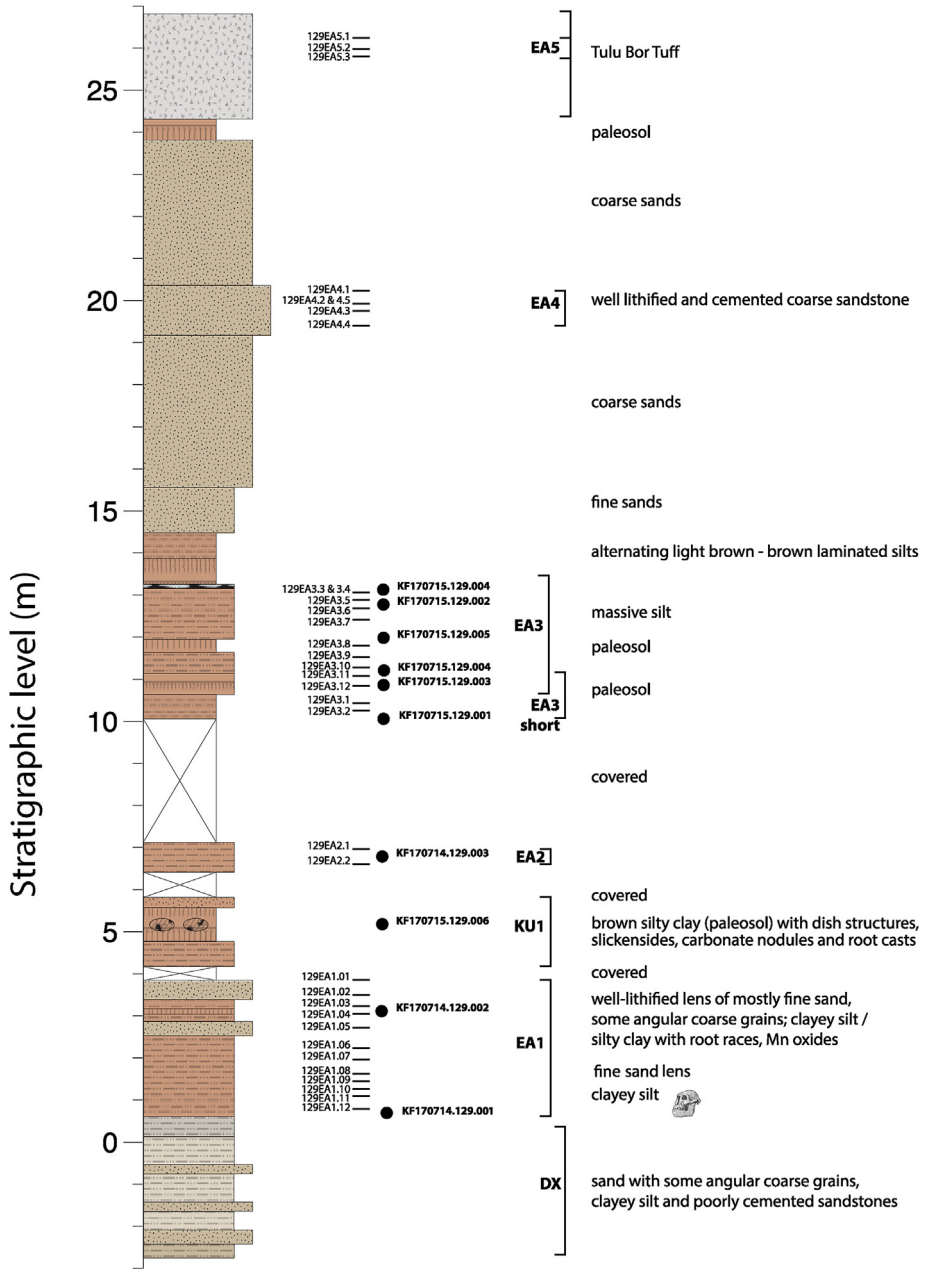

Figure 3. Paleomagnetic stratigraphic section with sediment descriptions and sample positions of both the paleomagnetic samples (EA-character strings) and the paleoecological samples (KF-character strings) from Area 129. The section approximately geographically equivalent to the NL129-17 section (in Fig. 2) relative to the hominin site, ET03-166/168.

regional mammal community dynamics associated with the hominin fossils.

1.4. Stable isotopes from vegetation proxies

Plant macrofossils are rare in the eastern African paleontological record, but geochemical signals from the terrestrial record provide reliable evidence of past vegetation. Stable carbon isotopes reflect how organisms physiologically utilize heavy and light stable isotopes. Typically, the stable carbon isotope signal of terrestrial organisms is determined by two functional groups of primary producers; grasses and sedges follow a C_4 photosynthetic pathway, while trees and shrubs follow a C_3 photosynthetic pathway. Plants using the crassulacean acid metabolism (CAM) pathway are also present throughout sub-Saharan Africa, but geographically restricted and productivity limited, and thus not discussed here (Ségalen et al., 2007; Monger et al., 2009). During photosynthesis, C_4 plants discriminate less against the heavier carbon isotope (^{13}C) and have a carbon isotope value ($\delta^{13}C$) that is more positive compared to C_3 plants (O'Leary, 1981). Carbon isotope ratios of the heavy to light carbon isotopes are expressed using delta notation, where $\delta^{13}C = [(R_{sample} - R_{standard})/R_{standard} - 1] \times 1000$ and $R = {}^{13}C/{}^{12}C$.

Each isotopic proxy for paleovegetation represents a different spatiotemporal signal of the paleoenvironment. Vegetation proxies utilized for stable isotope analysis vary from those derived directly from plant tissue (plant waxes) preserved in paleosol, to mineralized tissue (enamel) from mammalian herbivores who (during the time of enamel formation) consumed different proportions of plant types based on their dietary specializations, to pedogenic carbonate

nodules that formed from carbonates in soils over tens to hundreds of years and represent many generations of plants. Below, we introduce the three vegetation proxies used in this study.

Plants produce waxes, primarily on their leaf cuticles (outer coverings), to protect leaf tissue from abrasion by dust, attack from insects or fungi, and water loss from the leaf surface. Plant waxes include normal alkanes (*n*-alkanes) and *n*-alkanoic acids (fatty acids; Eglinton and Hamilton, 1967). Characteristic patterns in plant wax distributions can be used to identify plant-derived *n*-alkanes or fatty acids in the terrestrial sedimentary record, including lacustrine, fluvial, and paleosol sediments. The carbon isotope ratios of *n*-alkanes and fatty acids in these sediments reflect the photosynthetic pathways of local vegetation and can therefore be used to determine the proportion of C_3 and C_4 vegetation (Chikaraishi and Naraoka, 2001). Fatty acids and *n*-alkanes from C_3 plants have $\delta^{13}C$ values ranging from about −40 to −28‰; values in C_4 plants range from −24 to −18‰. Plant wax $\delta^{13}C$ values are more negative than their bulk plant tissue due to discrimination against ^{13}C during lipid synthesis (Chikaraishi and Naraoka, 2003). Fatty acids and *n*-alkanes are commonly preserved in sedimentary organic matter, where their resistance to diagenetic alteration and isotope exchange makes them an excellent geochemical proxy for reconstructing past vegetation. Biomarkers recovered from floodplain or pedogenic surfaces, as they are in this study, record a time-averaged but localized representation of the paleovegetation (Uno et al., 2016).

Pedogenic carbonates provide a different source of information about paleovegetation compared to plant waxes. Carbonate nodules that form at >30 cm below the soil surface typically reflect the isotopic ratios of C_3, C_4, or CAM plants present in soil rather than fluctuations in atmospheric CO_2 (Cerling, 1984). Each carbonate nodule represents a limited spatial (<1 m) but highly averaged temporal signal (10–1000 years) of the paleoenvironment (e.g., Behrensmeyer et al., 2007; Du et al., 2019). Pedogenic carbonates primarily form in semiarid environments, that is, seasonal environments with limited rainfall (<1000 mm of rainfall) (Cerling and Quade, 1993). Here, we combine published stable isotope values from Area 129 pedogenic carbonates as well as unpublished data from both the ET03-166/168 hominin site and the broader Area 129 region.

Stable carbon isotopes from enamel reveal the dietary breadth of an animal but can also be used as a proxy for paleovegetation. Carbon isotopes from enamel reflect the proportion of C_3, C_4, or CAM vegetation consumed by an individual during the development of their teeth (Cerling and Harris, 1999). While carbon isotopes indicate dietary specializations within taxa, at the community scale, carbon isotope values from a diversity of species can reveal large-scale shifts in vegetation availability, particularly in primary consumers with flexible diets, like bovids (e.g., Cerling et al., 1997, 2015; Lee-Thorp et al., 2007; Uno et al., 2011). Here, we examine carbon isotopes from the enamel of several large mammal taxa from Area 129 in East Turkana, primarily specimens associated with the ET03-166/168 site.

1.5. Phytoliths

Phytoliths are microscopic silica bodies that form in or around plant cells. They are preserved in soils after the plant's organic matter decays and can last for millions of years (Piperno, 2006). Phytoliths are classified using morphological features according to their anatomical origin, taxonomic affiliation, and/or functional traits (Twiss et al., 1969; Alexandré et al., 1997; Piperno, 2006; Strömberg et al., 2016). Some taxa produce specific identifier morphotypes, including grasses, palms, and sedges. Identification of grass phytoliths to subfamily level aids in reconstructing key ecological traits of the plant community (e.g., warm and humid, cool, hot and dry-adapted) and photosynthetic pathways (C_3 vs. C_4 grasses; Twiss, 1992; Strömberg et al., 2018). Phytoliths preserve well in multiple depositional environments (Albert et al., 2006, 2009; Barboni et al., 2010; Albert and Bamford, 2012). In paleosol and floodplain sediments, such as those examined in this study, phytoliths likely represent local but temporally averaged signals of vegetation biomass (Strömberg et al., 2018).

2. Materials and methods

2.1. Magnetostratigraphy and geochronology

All lithologies present at the NL129-17 section (Fig. 2) were sampled for magnetic polarity analysis except unlithified coarse sands (Fig. 3). Authors E.L.A., D.V.P., and M.J.S. collected 2.5-cm-diameter cylindrical rock cores with an electric drill mounted with a diamond-coated bit and cooled with an air-powered fan. Cores were oriented with a geological compass corrected for local declination. A total of 33 drilled samples were taken during the 2017 field season and cut to standard dimensions using a double-bladed saw. Magnetostratigraphic analyses were performed on 37 specimens from the 33 drilled samples to identify the transition from the Gauss to the Gilbert Chron (3.59 Ma) if present (Supplementary Online Material [SOM] S1 Methods; SOM Table S1).

2.2. Paleontological surveys

Over five field seasons in Area 129 (2003, 2012–2015), vertebrate fossil collection targeted the Lokochot Member (Figs. 1 and 2). Authors A.K.B, R.B., and A.V. used systematic biostratigraphic surveys to record and collect fossils (Behrensmeyer and Barry, 2005). The method prioritized collecting specimens with both taphonomic and paleoecological importance, including those that provide ecological insight, such as diversity and abundance (often craniodental remains), or accumulation processes (e.g., postcrania with carnivore damage). This collection methodology, referred to informally as 'bone walks' (BW), also aims to document all specimens that are not collected, from whole bones to unidentifiable fragments to trace fossils. The surveys use teams of trained paleontologists, and all specimens were identified to the most specific taxonomic level possible in the field. Only specimens visible on the surface of outcrops were recorded during these systematic surveys. Specimens that provided higher-resolution (tribe to species level) taxonomic and taphonomic information were collected, locations were recorded using high-resolution (~3 m buffer) GPS and are curated in the Palaeontology and Archeology Divisions of the Earth Sciences Department at the National Museums of Kenya. Geographic and geologic context were recorded using field geospatial data collectors (GISPro on an iOS device) and stratigraphic sections. All specimens have barcode IDs and are recorded in the Koobi Fora Research and Training Program database.

These collections were augmented using a 'surface scrape' methodology at the ET03-166/168 site, where hominin fossils were recovered. The top layer of sediment was removed and screened through a 3-mm sieve. All fossils identifiable to tribe level were collected and cataloged. Data from the biostratigraphic survey and surface scrapes complement material from typical fossil collection methods used in previous seasons, which often focused on concentrations or 'patches' of fossils. These patches typically represent specific taphonomic circumstances favorable to fossil preservation (Behrensmeyer et al., 2000), whereas biostratigraphic surveys represent the broader fossil landscape for particular stratigraphic intervals.

Systematic biostratigraphic sampling is limited to single, well-defined stratigraphic horizons, providing a measure of the distribution of fossils on the outcrop surface, which can also reflect their original distribution in different paleoenvironments on the ancient landscapes (Behrensmeyer and Kidwell, 1985; Behrensmeyer and Barry, 2005). In Area 129, the well-defined blocks of stratigraphic horizon extended from the base of the outcrop representing the modern Il Naitirwa drainage to the top of the Lokochot Member, which is capped by the distinctive outcrop of the Tulu Bor Tuff. The surveys reported in this study were conducted within ~1 km of the primary stratigraphic reference section, NL129-17 associated with the ET03-166/168 site, which occurs in the silty sand at the base of NL129-17 (Fig. 2). The strata represented in the NL129-17 section were initially surveyed and fossils collected in 2003, with subsequent fossil collections in 2012, 2013, 2014, and 2015. A microstratigraphic section by A.K.B. in 2003 (AKB129-BW68) shows the detail at the ET03-166/168 hominin site (Fig. 2). The specimens collected between 2003 and 2015 have higher-resolution metadata compared to those recovered before 2003, including more spatially and stratigraphically explicit information. Previous (pre-2003) field collections as well as specimens from our systematic surveys are combined for regional faunal comparisons (specimen-level data are available in a GitHub repository at https://github.com/ameliavillasenor/Area-129-manuscript). Contextual information such as substrate, slope, and outcrop conditions were recorded for each surveyed fossil occurrence.

New hominin specimens were recorded during systematic surveys in Area 129 beginning in 2003. Morphological descriptions of the fossil hominin material can be found in SOM S2 Results.

2.3. Faunal abundance

Faunal abundance analyses of East Turkana were limited to specimens associated with the Lokochot Member (~3.6–3.4 Ma). We examined both the proportions of taxa identified to family in the Area 129 sample as well as those within ~50 lateral meters of the same silty sand unit as the primary hominin site ET03-166/168 (https://github.com/ameliavillasenor/Area-129-manuscript).

For a broader geographic comparison of medium-large mammals (>1 kg), we also included roughly contemporaneous specimens from equivalent strata in the Nachukui Formation (West Turkana) and the Hadar (Awash Valley, Ethiopia) and Shungura (Lower Omo Valley, Ethiopia) Formations. Proportions of specimens were compared between East Turkana (Areas 129 and 117), West Turkana, the Lower Omo Valley, and Hadar/Dikika at family and tribe taxonomic levels. Mammal specimen lists that are attributed to members dated between 3.60 and 3.44 Ma were compiled from an updated and unpublished version of the Turkana Basin database (East Turkana data, updated in 2015; West Turkana data, updated 2003; Bobe, 2011; https://github.com/ameliavillasenor/Area-129-manuscript), the Hadar database, and published contemporaneous Dikika fauna (updated in 2011; available upon request to Christopher Campisano; supplemented with data from Reed and Campisano, 2012 and Bedaso et al., 2013), and the Omo database (updated in 2003; Bobe and Eck, 2001; Alemseged et al., 2007; Eck, 2007; https://github.com/ameliavillasenor/Area-129-manuscript). The open nomenclature modifiers ('cf.' and 'aff.') were excluded from taxonomic assignments, although we recognize that this includes specimens of unconfirmed identity at higher levels of taxonomic resolution. To standardize specimen counts among databases, specimen numbers were used to count the number of identifiable specimens (NISP). Though sampling protocols at each site varied, all favored the preferential recovery of craniomandibular remains of large mammals (>1 kg and <1000 kg), particularly primates and carnivorans (Villaseñor et al., 2020). Furthermore, though the four sites (East Turkana, West Turkana, Omo, and Hadar/Dikika) represent a range of depositional environments through time, all exhibit fluvial accumulation within their deposits (Villaseñor et al., 2020). Fluvial units represent large time (10^2–10^4 years) and spatial scales (Behrensmeyer, 1988). Since this comparison averages these large scales of fossil data, we interpret the interbasin mammal community comparisons as regional-scale environmental indicators. This is in contrast to the local-scale paleoenvironmental indicators represented by the paleoenvironmental data from ET03-166/168.

The bootstrap method described in Villaseñor et al. (2020) was used to calculate 95% confidence intervals for each taxon (tribe or family) within each site (Efron and Tibshirani, 1994; Manly, 2007). This method reflects the uncertainty in abundance when the sample size is small. Bootstrapping and quantile functions were conducted in R base package v. 4.1.2 (R Core Team, 2021).

2.4. Plant wax biomarkers

Ten sediment samples were collected during field work in 2017 by K.T.U. and E.L.A. for biomarker, phytolith, and soil carbonate analyses (SOM S1; SOM Table S2; Fig. 3). The samples were collected from the vertical section (NL129-17) associated with the hominin site (ET03 166/188). Sediment samples containing pedogenic carbonates were analyzed for $\delta^{13}C$ (described in section 2.5). The sediment sampling protocol was designed to avoid potential contamination from modern plant waxes, with all samples collected from newly excavated trenches in areas with little or no overlying vegetation. Nitrile gloves prevented contamination from modern sources of lipids. About 300–500 g of freshly exposed, consolidated sediment was collected directly onto aluminum foil from 25 to 55 cm below the modern land surface. Prior to wrapping in foil, the samples were inspected for any traces of modern roots or plant matter. Carbon isotope ratios of *n*-alkanes and fatty acids of plant waxes were prepared by K.T.U. and analyzed using a GC coupled to a Thermo Delta V isotope ratio mass spectrometer through a combustion interface at the Lamont Doherty Earth Observatory Stable Isotope Laboratory (SOM S1).

Carbon isotope data were corrected following the methods outlined in Polissar and D'Andrea (2014) using a MATLAB (MathWorks; Natick, MA) routine. Error is presented as the standard error of the mean and includes uncertainty in the reference gas, multiple injections, and standard values. To compare with the other carbon isotope data sets in this study, C_{31} *n*-alkane carbon isotope data were converted to % C_4 values based on a linear mixing model with endmembers defined by a large data set of modern African plants compiled by Polissar et al. (2021). After adjusting endmembers by +1.7‰ to account for changes in the $\delta^{13}C_{atm}$ from modern (−8.0‰) to preindustrial values (−6.3‰; Francey et al., 1999), we arrive at −32.4 ± 2‰ for the C_3 and −20.0 ± 2‰ for the C_4 endmembers, respectively. There is no correction for the $\delta^{13}C$ values of atmospheric CO_2 ($\delta^{13}C_{atm}$) between the Pliocene values from Area 129 (3.59–3.44 Ma), estimated to be −6.2‰, and the commonly accepted preindustrial (1750 AD) value of −6.3‰ (Francey et al., 1999). The difference in the two values is similar to the uncertainty of the isotopic measurement and smaller than the uncertainty in the reconstructed Pliocene values (0.35‰) determined by Tipple et al. (2010).

2.5. Pedogenic isotopic analysis

Fifty pedogenic carbonate samples were collected from Area 129 between 2003 and 2017, including seven from within the NL129-17 section and its equivalent paleomagnetic section (Figs. 2 and 3; SOM Table S3). These seven samples represent the 20 vertical

meters measured from the hominin-bearing silt (ET03-166/168), which is at the base of the NL129-17 section (Fig. 2). Twenty-seven of the 50 samples were previously published (SOM S1; SOM Table S3; Levin et al., 2011). Pedogenic carbonates were collected from sediments that show clear evidence of pedogenesis (e.g., dish structures, root casts) and derive from largely clay-rich contexts. All pedogenic carbonate samples were collected from below the Tulu Bor Tuff. Each sample was collected from a trench extending at least 40 cm below the top of the soil formation (Levin et al., 2011). Only soil samples with discrete nodules were sampled, and 1–2 nodules were analyzed per soil horizon (SOM S1).

We compiled the new East Turkana data with published values from East Turkana with estimated ages of 3.60–3.44 Ma. East Turkana $\delta^{13}C$ values were also compared to published Hadar and West Turkana $\delta^{13}C$ values from this time interval (Levin, 2013). West Turkana data were updated with values from Lomekwi (Harmand et al., 2015).

To compare Area 129 stable isotope data sets from the different proxies (leaf wax biomarkers, enamel, and soil carbonate), carbon isotope data were converted to % C_4 values using a linear mixing model as described in Cerling et al. (2015). The linear mixing model used $\delta^{13}C$ endmember values from both mesic and xeric vegetation systems (Cerling et al., 2015). End members are based on estimates of $\delta^{13}C$ values for C_3 and C_4 vegetation corrected to preindustrial (1750 AD) values: mesic estimates are −26.6‰ for C_3 and −11.2‰ for C_4 endmembers, while xeric estimates are −25.6‰ for C_3 endmembers and −10‰ for C4 endmembers. As with the plant wax isotopes, we made no adjustment between $\delta^{13}C_{atm}$ values from the Pliocene (−6.2‰) and preindustrial periods.

2.6. Enamel isotopes

We obtained enamel from large mammal herbivores ($n = 45$) associated with the Lokochot member in Area 129. The specimens were collected during the 2003–2015 field seasons during systematic biostratigraphic surveys (Behrensmeyer and Barry, 2005) in Area 129. Specimens were identified to the most specific taxonomic level possible by A.V., R.B., and A.K.B. Each specimen was assessed for signs of diagenesis (e.g., recrystallization on tooth surfaces). Nonaltered specimens were sampled using a diamond-tipped drill bit after removing several microns of surface enamel. Stable carbon isotopes were analyzed from Area 129 specimens identified to at least the family level (Cerling et al., 2015; SOM S1; Table S3).

Using the same endmember estimates for mesic and xeric systems applied to pedogenic carbonates, enamel $\delta^{13}C$ values were converted to % C_4 values using a linear mixing model (Cerling et al., 2015). These C_4 estimates provide the basis for comparing isotopes from enamel with other carbon isotope data sets from different proxies. Enamel is assumed to be 14‰ enriched compared to vegetation (Cerling and Harris, 1999).

2.7. Phytoliths

The 10 sediment samples described in section 2.4 were also processed and analyzed for phytoliths following the Strömberg et al. (2013) protocol (SOM S1). At least 200 diagnostic phytoliths were counted for each sample to ensure robust environmental reconstructions (Albert and Weiner, 2001; Strömberg, 2009). Author R.K. classified diagnostic phytoliths into three main categories based on the functional types of plant habitats: (1) grasses include diagnostic taxa such as Panicoideae, Chloridoideae, and unidentified PACMAD (Panicoideae, Aristidoideae, Chloridoideae, Micrairoideae, Arundinoideae, and Danthonioideae) lineages; (2) the 'woody' category of phytoliths represents plants associated with closed habitats, which include trees and woody dicot morphotypes, whereas 'dicot general' includes a wider range of taxa, including shrubs and herbaceous plants; and (3) palms consisting of diagnostic echinated palm phytoliths (SOM Fig. S1). Nondiagnostic phytoliths were classified as 'others' (Strömberg, 2003).

Two environmental indices were calculated from a subset of phytolith morphotypes: the Dicotyledons/Panicoideae (D/P) and Iph (the ratio of Chloridoideae [saddle] morphotypes over the sum of Panicoideae [bilobates + crosses + polylobates] and Chloridoideae phytolith types; Bremond et al., 2008a). The Iph index estimates the moisture gradient, where a higher Iph index indicates higher aridity, while lower values indicate more humid-adapted grasses and lower aridity (Bremond et al., 2008b). Chloridoideae phytolith types are primarily found in hot and dry climates at low elevation, while Panicoideae (which primarily uses the NADP-me pathway) is associated with warm and moist climates (Twiss, 1992; Cerling and Harris, 1999; Peterson et al., 2010).

The D/P phytolith index is a ratio of the tree-derived phytolith type (dicotyledons; spheroid granulate morphotypes) over the sum of Panicoideae-derived (bilobates + crosses + polylobates) morphotypes. The D/P index is thus a coarse indicator of tree density, where higher values indicate more trees. This index correlates well with the leaf area index, and both are good indicators of the forest-to-savanna transitions (Bremond et al., 2005).

3. Results

3.1. Geochronology

Characteristic remanence magnetization directions are normal, and no reversal has been identified (SOM S2). Since the sedimentary layers sampled here are capped by the Tulu Bor Tuff, which has been dated to 3.44 ± 0.041 Ma, the normal direction found throughout the section supports our expectation that the sediments sampled in this study fall within the Gauss chron2An (C2An;

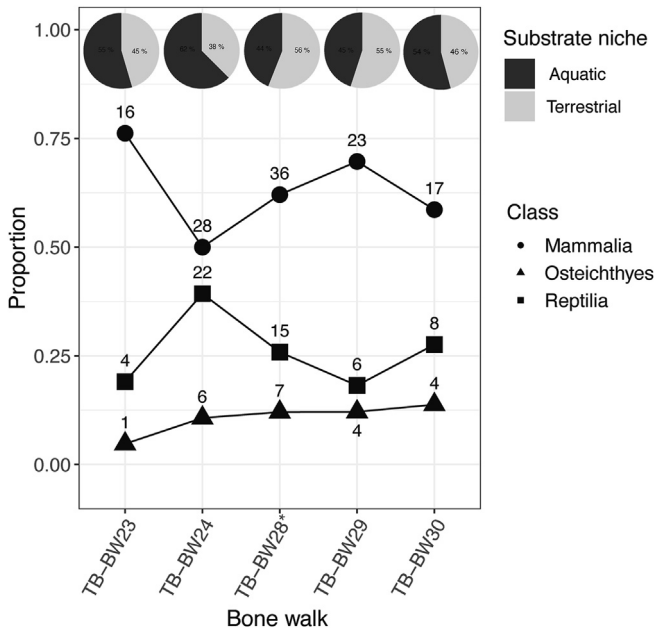

Figure 4. Five systematic surveys ('bone walks') with the largest fossil samples ($n > 20$ specimens), all representing the Lokochot Member stratigraphic interval shown in Fig. 2. Pie charts show the percent of specimens that can be identified as aquatic or terrestrial. Line graphs show the percent of class-level taxa from each bone walk (BW). The asterisk associated with BW-28 indicates that the survey is associated with the hominin fossil level. Bone walk-29 and 30 are within 100 m of the hominin site (TB-BW28). Note BW 28 and 24 are most fossiliferous.

2.61–3.596 Ma). We did not identify the transition from the Gauss to the Gilbert Chron (3.596 Ma), suggesting that all sediments in this study are younger than 3.596 Ma. Based on this evidence, the age of the hominin locality is inferred to be between ~3.596 and 3.44 Ma.

3.2. Paleontological survey

Five systematic surveys from Area 129 conducted within 1 km of the primary hominin site (ET03-166/168) yielded sample sizes of >20 specimens. Two (TB-BW24 and TB-BW28) were particularly fossiliferous (>56 specimens), but only TB-BW28 was diverse, with nine different orders of vertebrates, including a hominin specimen recovered during the initial survey (Fig. 4). Both TB-BW28 and the nearby TB-BW29 showed higher percentages of mammalian and terrestrial vertebrates than the other nearby surveys (Fig. 4). The targeted surveys near the primary hominin-bearing site (TB-BW28) revealed a diverse mammalian community within a small area, where clusters of small nonhominin primate specimens ($n = 6$) were found in association with the (ET03-166/168) hominin locality. Three of the four hominin specimens (KNMER-72590, 72591, and 71396) and many other mammal fossils were derived from bone walks conducted in 2003 (data included here) and 2012–2015 (data not included here).

3.3. New hominin specimens

The new hominin fossils consist of an upper premolar crown and three partial molars (SOM S2; Fig. 5). The ET03-166/168 Area 129 hominin premolars and molars are morphologically consistent with all contemporaneous hominin fossils from eastern Africa to which they can be compared, which derive from Lomekwi, Hadar, Maka, and Woranso Mille (Leado Dido'a area; White et al., 2000; Leakey et al., 2001; Melillo et al., 2021). In size, the premolar crown (KNM-ER 72592) falls within the range of P^{3}'s of *A. afarensis* from Hadar, Ethiopia, and teeth from Lomekwi, Kenya, which are unattributed to taxon but are found from deposits that have yielded *K. platyops* (Leakey et al., 2001; Skinner et al., 2020). KNM-ER 72592 is slightly smaller than the two specimens attributed to *Australopithecus deyiremeda* from Woranso Mille (SOM Table S4). The only molar that can be measured (KNM-ER 72951) falls within the size range for molars from all three comparative samples. The Area 129 hominins are not diagnostic to a particular taxon given their preservation and the fact that, to date, no diagnostic features of upper premolar or molar crowns preserved in the Area 129 specimens discriminate among *A. afarensis, A. deyiremeda*, and the Lomekwi hominins (Skinner et al., 2020; Melillo et al., 2021).

Figure 5. KNM-ER 72590 (M^1 or M^2) shown in mesial view, KNM-ER 72591 (right M^1) and KNM-ER 72592 (left P^3) shown in occlusal view, and KNM-ER 71396 (M^1 or M^2) shown in mesial view.

3.4. Faunal abundance

The proportions of mammal fauna in Area 129 (Fig. 6) are similar to the broader Pliocene East Turkana region's mammalian proportional abundance, where bovids, cercopithecids, and suids comprise the most abundant groups (Fig. 7). The Area 129 sample contains the only hominin fossils from the Lokochot Member on the east side of Lake Turkana. The ET03-166/168 site, where most of the hominin specimens were recovered, contains a greater proportion of primate (26%) and hominin specimens (3%) compared to the larger Area 129 or East Turkana region (Figs. 6 and 7; SOM S1; SOM Table S5).

Between 3.44 and 3.60 Ma, in the Afar and Turkana Basin sites discussed here, bovids are the most abundant large mammal group except in the Lower Omo Valley, where suids are most abundant (Fig. 7). East Turkana has the greatest proportion of cercopithecid specimens (14% of the total; Fig. 7), and the newly discovered

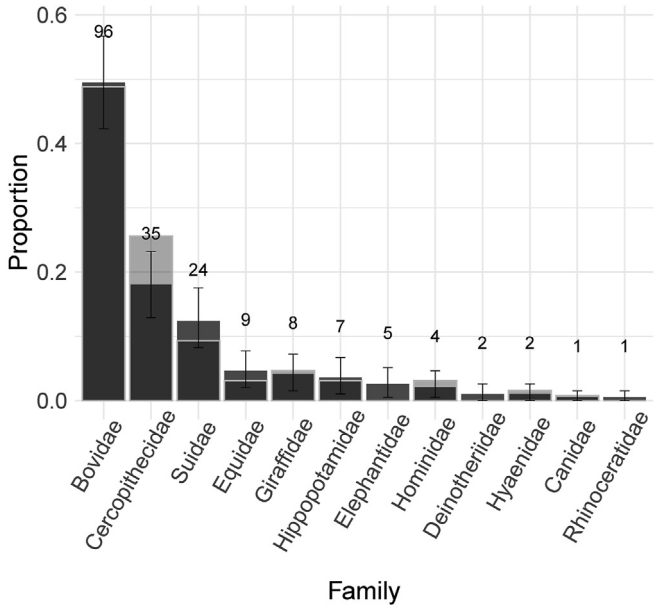

Figure 6. Mammal (>1 kg) family abundance from Area 129 (3.59–3.44 Ma; individuals based on database specimen numbers). Light gray bars indicate the proportion of taxa that are spatially associated (within ~50 m) with hominin site and stratigraphic section ET03-166/168 (SOM Table S5). Notably, there is a higher proportion of Cercopithecidae associated directly with the hominin site.

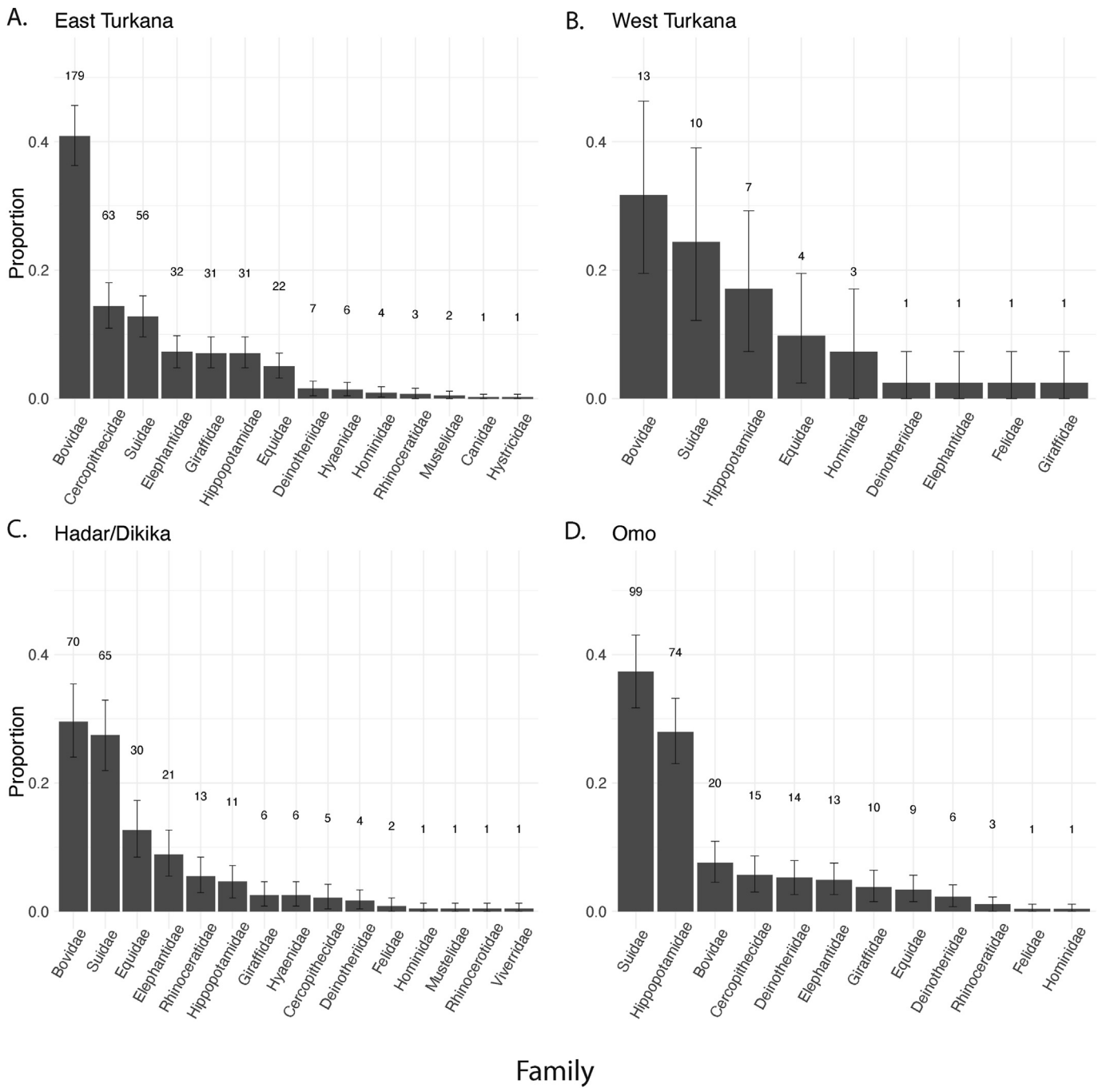

Figure 7. Family abundance (individuals based on database specimen numbers) from sites representing the Lokochot member and (approximate) age equivalent sediments in the Turkana and Afar basins, including East Turkana ($n = 438$), West Turkana ($n = 41$), Hadar ($n = 237$), and the Lower Omo Valley ($n = 265$). Data are based on published, catalog, and other sources of information described in the text and Villaseñor et al. (2020). East Turkana includes new data from this study, combined with accessioned data from the Turkana Basin (https://github.com/ameliavillasenor/Area-129-manuscript).

hominins comprise ~1% of the total specimens identified to family. In contemporaneous sediments of Hadar/Dikika and the Lower Omo Valley, hominins make up less than 1% of the sampled mammal community; large herbivore families are the most abundant groups at these sites. In contrast, hominids are 7% of the large mammal fauna recorded in West Turkana. However, the total sample size of mammals attributed to family within West Turkana's Kataboi Member (=Lokochot) is very low ($n = 41$), compared to the other three equivalent formations with >250 specimens each (Fig. 7).

The cross-basin comparison at the tribe level shows that East Turkana diverges from West Turkana, the Lower Omo Valley, and Hadar/Dikika (Fig. 8). Nyanzachoerini is the most abundant tribe identified in the Lower Omo Valley, Hadar/Dikika, and West Turkana (>27% among all sites). The Lower Omo Valley has more than 60% of its specimens attributed to Nyanzachoerini, and the second most abundant tribe is Papionini. East Turkana contains the lowest proportion of Nyanzachoerini (13%), and Alcelaphini and Tragelaphini are as abundant as Nyanzachoerini. West Turkana has only 30 specimens identified to the tribe level, making

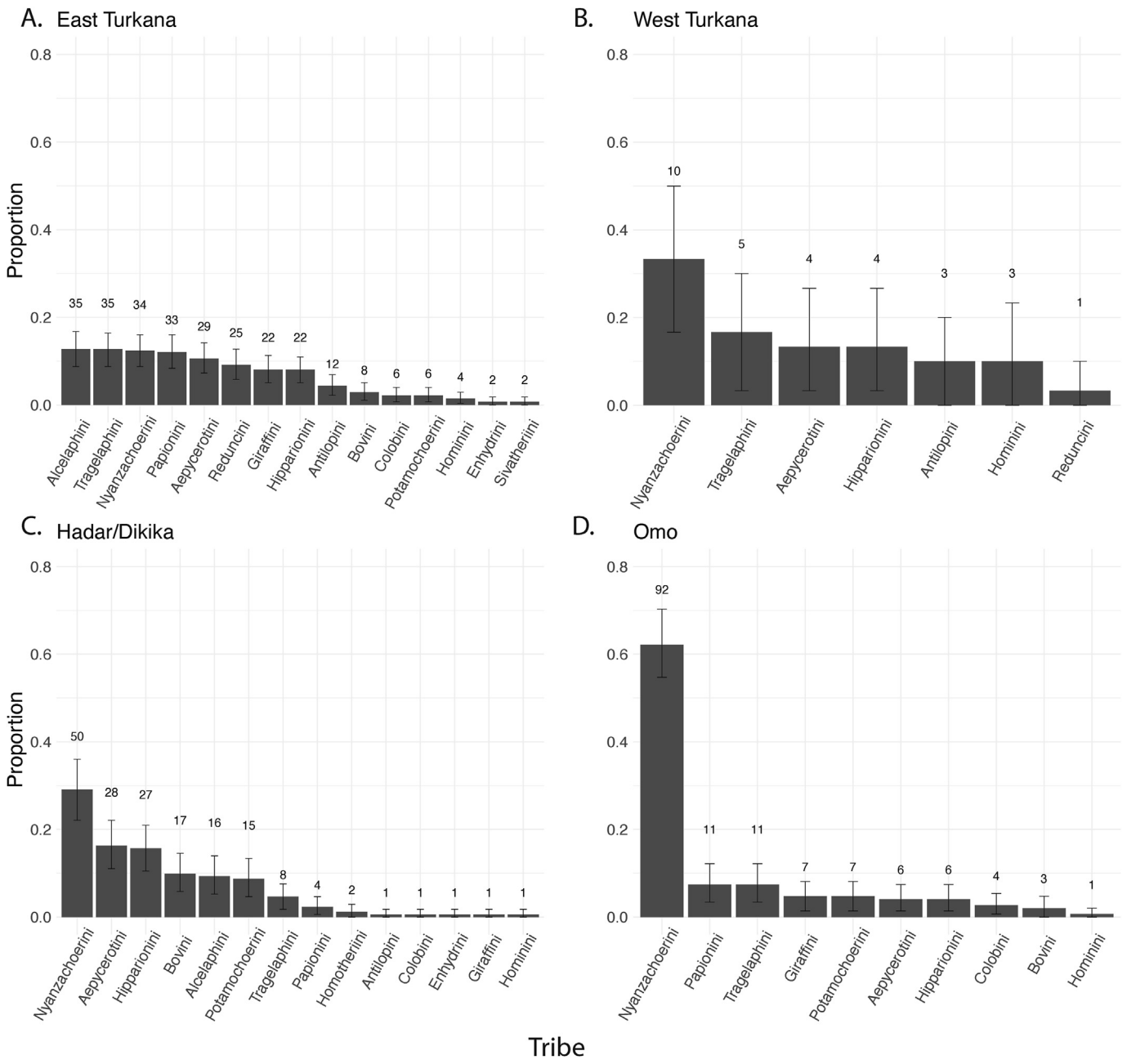

Figure 8. Tribe abundance (individuals based on database specimen numbers) from sites representing the Lokochot member and equivalent sediments in the Turkana and Afar basins, including East Turkana ($n = 275$), West Turkana ($n = 30$), Hadar ($n = 172$), and the Lower Omo Valley ($n = 148$). Data are based on published, catalog, and other sources of information described in the text and Villaseñor et al. (2020). East Turkana includes new data from this study, combined with accessioned data from the Turkana Basin (https://github.com/ameliavillasenor/Area-129-manuscript).

comparisons with better sampled regions uncertain. Both East Turkana and Hadar/Dikika are more taxonomically diverse than the Lower Omo Valley or West Turkana. They also have more even proportions of taxa, with no tribe representing more than 27% of the assemblage.

3.5. Plant wax biomarker concentrations and $\delta^{13}C$

Chemical analyses indicated good preservation of plant wax biomarkers in the terrestrial soils of Area 129 (SOM S1; SOM Tables S6 and S7). We focus on the C_{31} *n*-alkane and corresponding C_{30} fatty acid (*n*-alkanoic acid) $\delta^{13}C$ data because the C_{31} *n*-alkane is produced in relatively similar abundances by C_3 and C_4 plants and therefore makes it the best representative of paleovegetation (Garcin et al., 2014). C_{31} *n*-alkanes ($n = 6$) range from −27.2 to −22.9‰ (SOM S2; SOM Table S8). The C_{30} fatty acids (*n*-alkanoic acid; $n = 8$) show a slightly wider range in $\delta^{13}C$ values from −30.3 to −21.8‰ (SOM S2; SOM Table S9). There is strong agreement between the two *n*-alkyl lipid homologs (C_{31} *n*-alkanes and C_{30} fatty acids), further supporting the isotopic integrity of the plant waxes. The calculated % C_4 values from the C_{31} *n*-alkane range from 42 to 76% C_4 (median = 46 ± 23% C_4; Fig. 9). Plant wax $\delta^{13}C$ data from within the hominin-bearing horizon indicate an average of 49 ± 24% C_4 vegetation (Fig. 10).

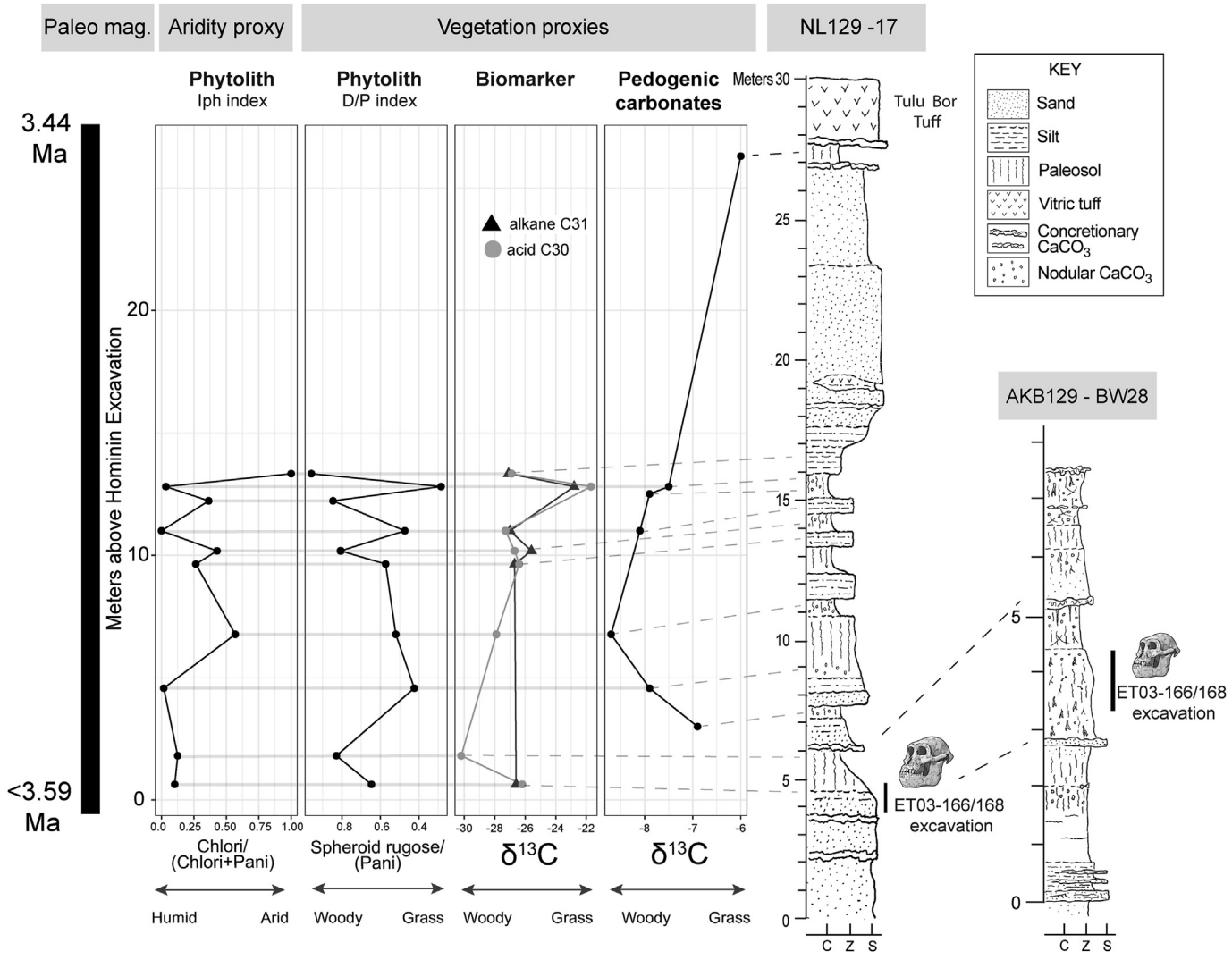

Figure 9. Multiproxy comparison of paleoecological data through the Lokochot Member section (NL129-17) at the ET03-166/168 site. From left to right: Paleo mag. = paleomagnetic signal representing all normal polarity, with no magnetic reversals detected; Aridity proxy = Iph index from phytoliths; Vegetation proxies = estimates of tree density from phytoliths (D/P index); $\delta^{13}C$ signals from plant wax biomarkers (C30 and C31) and pedogenic carbonates. The hominin specimens and the majority of other faunal remains from this area were recovered from a pedogenically modified silty sand and clayey silts near the base of NL129-17. Section AKB129-BW28 shows detailed stratigraphy at the hominin site and inferred correlation of the source sediments to the NL129-17 reference section. Lateral variation in the fluvial lithofacies is represented in the differences between the proportions of sands and thicknesses of paleosols of the two sections. Dashed lines show the stratigraphic positions of paleoecological proxy samples in the NL129-17 reference section, based on field correlations by K.T.U., D.V.P., and M.J.S. Light gray lines connect contemporaneous proxies, representing samples from the same source bed.

3.6. Pedogenic carbonate $\delta^{13}C$

The range of $\delta^{13}C$ values from the NL129-17 section ([−8.7‰] – [−6‰]) indicates vegetation that ranges from moderate to high woody cover in fluvial floodplain environments (Figs. 9 and 10). The average $\delta^{13}C$ of Area 129 (−7.02‰) is indistinguishable from the larger coeval East Turkana regional signal for the middle Pliocene (−7.1‰), based on published values from the Area 117 region to the southwest (Levin et al., 2011). Across Area 129, values range from −8.7 to −4.3‰. The average values are concordant with contemporaneous Hadar and West Turkana $\delta^{13}C$ average values (−7.3‰ and −7.4‰, respectively). Slightly more positive $\delta^{13}C$ values in the East Turkana region suggest that the paleolandscape maintained less woody cover than coeval samples from West Turkana or Hadar. Compared to the C_4 biomass represented by enamel and plant wax biomarkers, pedogenic carbonates from both NL129-17 (12–31% C_4) and the larger Area 129 (13–43% C_4) represent significantly less C_4 biomass (Fig. 10).

3.7. Enamel $\delta^{13}C$

The large herbivore families of Area 129 are primarily mixed (C_3–C_4) feeders or C_4 vegetation specialists (Fig. 10; SOM Table S10). At the ends of the $\delta^{13}C$ dietary spectrum are Giraffidae (a C_3 specialist with mean $\delta^{13}C = -12.0‰$) and Equidae (a C_4 specialist with mean $\delta^{13}C = -1.1‰$). Suidae consumed primarily C_4 biomass (average $\delta^{13}C = -2.1‰$). The largest sample of herbivores is from the family Bovidae ($n = 26$), which also skews toward the C_4 end of the spectrum ($\delta^{13}C = -2.8‰$). The average % C_4 estimate from the large mammal community (using the mesic endmember estimates) is 61–63%. Using xeric endmember estimates, the estimate for the large herbivore community is 86–93% C_4. Thus, carbon isotopes from enamel suggest C_4 biomass consumption was high using either endmember when compared to the vegetation proxies, especially pedogenic carbonates. Pedogenic carbonates suggest at most 43% C_4 biomass on the landscape, which is much lower

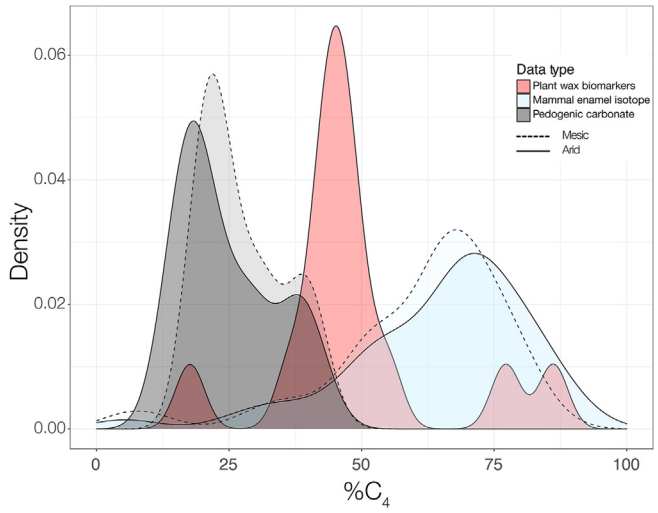

Figure 10. $\delta^{13}C$ values were transformed into % C_4 estimates for plant wax biomarkers, mammal enamel isotopes, and pedogenic carbonates. The data are presented as probability density functions of the % C_4 estimates. Endmember estimates from xeric and mesic ecosystems are represented by solid and dashed lines, respectively. Despite slight variation between these estimates, the % C_4 differences represented by mammal enamel, plant wax biomarkers are maintained and suggest potential biases associated with these different proxies. (For interpretation of the references to color in this figure legend, the reader is referred to the Web version of this article.)

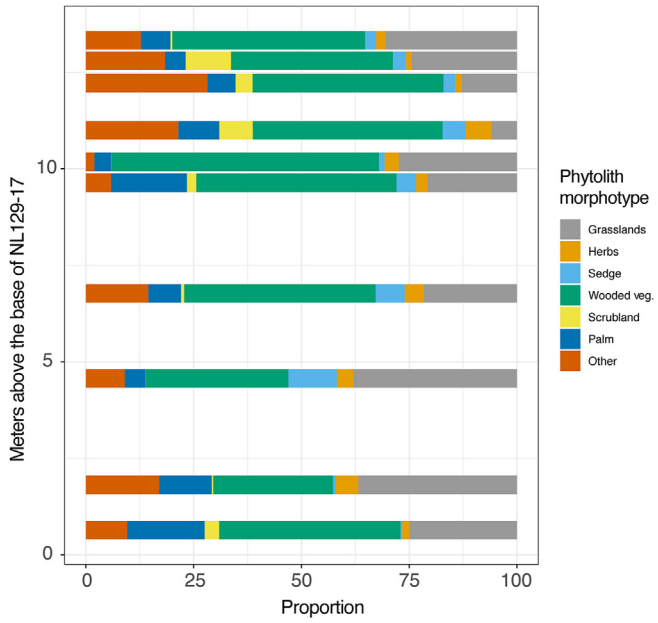

Figure 11. Phytolith morphotype proportions from the section (NL129-17) associated with the ET03-166/168 hominin locality. (For interpretation of the references to color in this figure legend, the reader is referred to the Web version of this article.)

than would be inferred from the large herbivore community $\delta^{13}C$ diet (Fig. 10).

3.8. Phytolith analysis

Through time (across the 10 samples from the NL129-17 section), the phytolith assemblage is dominated by forest indicator and woody dicot morphotypes, followed by grass short silica cells (GSSCs) phytoliths (Fig. 11; SOM Table S11). The average distribution of identifiable phytoliths across the 10 samples in the NL129-17 section was 42.7% woody (including both forest indicator phytoliths and woody dicots) and 24.3% grass (SOM Table S11). Palm and sedge diagnostic morphotypes were also present throughout the section, ranging from 3% to 18% and 1% to 5%, respectively. Morphotypes that were nondiagnostic to specific plant functional types were categorized as general dicots. The GSSCs phytoliths show the grasslands consisted of both tall Panicoideae and short Chloridoideae C_4 grasses and other unidentified PACMAD grasses.

4. Discussion

4.1. Area 129 hominins were associated with a diverse primate community and riparian environments

Phytolith data associated with the hominin level suggest vegetation consisting of large proportions of wooded vegetation (D/P index) and humid-adapted C_4 grasses (Iph index; Fig. 9). The primary hominin-bearing layer is a sandy silt capped by a paleosol. Plant wax biomarkers and phytoliths were recovered from the upper portion of the sandy silt unit, near the boundary between the hominin-bearing layer and the overlying paleosol (~0.64 m above the base of the fossil-bearing silty sands; Fig. 3). In this layer, woody plants and palms comprise nearly 60% of the recovered phytoliths, while C_4 vegetation comprises approximately 20% of the remaining sample (Fig. 11; SOM Table S11). Sedges and palm phytoliths indicate the presence of swampy and/or wetland habitats on the fluvial floodplain. Specifically, forest tree–derived morphotypes and palm morphotypes reflect forest vegetation associated with riparian or freshwater habitats, respectively (Ashley et al., 2009; Barboni et al., 2019). A small proportion of scrubland phytoliths (3%) from this layer suggest occasional or proximal arid conditions. Plant wax biomarker data support a mixed wooded-grassland environment with 49% C_4 vegetation (mean for samples from the hominin level). Phytolith data indicate that the C_4 component was composed of grasses and sedges.

Sedimentary features in Area 129 also provide evidence that freshwater habitats were regularly present, supporting the paleovegetation reconstructions. The vertical pattern of sands, finer silts, and clays with pedogenic modification, capped again by sand, recorded in the NL129-17 section is typical of aggrading fluvial systems in which a channel moves laterally across its floodplain over time (e.g., Smith and Putnam, 1980). Aggrading fluvial systems build fining-upward sequences from sand to stacked units of silt and clay, which are then capped by another sand, representing the return of the channel to this part of the alluvial plain. The thick sandstone between meters 17.5 and 26 (just below the Tulu Bor Tuff) represents a channel of considerable size, likely a major river for Pliocene East Turkana. Some of the surface fossils recorded in the systematic bone surveys may be derived from these sands. Active channels and proximal floodplains represent unstable land surfaces for vegetation, but fluvial systems also support nearby regions with stable surfaces with extensive soils and perennial vegetation, such as trees. The presence of large channels may explain the large proportion (44% and greater) of aquatic animals recorded during systematic bone surveys (Fig. 4), which in turn support the hypothesis that bodies of water, such as perennial channels and associated floodplain wetlands, were present within kilometers of the ET03-166/168 hominin locality. The combined evidence thus indicates that the hominins at ET03-166/168 were preserved in a floodplain landscape that supported riparian vegetation and a diverse mammalian community.

The sample of mammals spatially associated with the new hominin fossils contains a large proportion of primates, primarily small cercopithecids (26% of the mammalian community) (Fig. 6), which is higher than the overall collection from Area 129 and East

Turkana. Small-sized cercopithecids, such as guenons, likely incorporated C_4 resources into their diets by the middle Pliocene (Levin et al., 2015; Manthi et al., 2020), but these species are usually somewhat arboreal and associated with wooded regions (Frost et al., 2020). Reed (2008) found that modern forest communities (generally associated with >1000 mm of rainfall) are composed of nearly 20% species with arboreal adaptations, while closed woodlands and ecotones (forest edge environments) have nearly 10% of community members with arboreal adaptations. If the NISP tallies of a relatively small assemblage ($n = 129$) provide some indication of original abundance in the original ecosystem, the faunal assemblage associated with the hominin fossils includes an unusual number of arboreal species. This suggests that the fossil assemblage represents a mammalian community associated with woodlands, such as a gallery forest or groundwater-fed wetlands (Barboni et al., 2019). The unusual representation of small primate specimens may also be the taphonomic signature of a bone-accumulating agent such as a large raptor or mammalian carnivore (Fernández-Jalvo et al., 2016). One of the primate teeth collected from the site shows evidence of enamel dissolution that supports this hypothesis (Fernández-Jalvo and Andrews, 2016).

Assuming paleolake Lokochot was present to the west, the larger-scale paleoenvironment recorded in Area 129 can be reconstructed as a broad, heterogeneous alluvial plain with river channels, seasonally flooded low areas, and an emergent, productive floodplain area that merged farther westward into a fluvial-deltaic plain. Upland and drier terrestrial landscapes may have been present to the east. The riparian environments bordering Lake Turkana likely had limited drainage basins that supported local ecosystems distinct from those of the larger paleo-Omo River to the north, where hominin fossils are rare at this time (Villaseñor et al., 2020). The Lower Omo Valley River deposits represent a perennial channel system and an extensive drainage basin in the Ethiopian highlands. This large river system supported dense riparian woodlands inhabited by larger numbers of suids and C_3-consuming bovids than are present in contemporaneous East Turkana, in addition to large numbers of cercopithecids (Figs. 6 and 7; Barr, 2015; Negash et al., 2020). By contrast, evidence from vegetation proxies and the mammalian community spatially associated with the Area 129 hominin fossils suggests that these hominin fossils were associated with a mix of wooded and riparian habitats with mesic grasses. Sedimentary evidence from the upper sections of NL129-17 indicates alternating periods of flooding and aridity associated within a variable and possibly ephemeral fluvial regime. In summary, the depositional, fossil, and vegetation information indicate that the Area 129 hominins and other fauna inhabited a floodplain landscape with humid grasses and substantial C_3 biomass.

4.2. Vegetation proxies show major ecological shifts over time within a single site

Contemporaneous vegetation proxies are preserved within ~17 m above the base of the section within a series of alternating paleosols, bedded silts, and sandy silts, which indicate that stable floodplain surfaces were periodically interrupted by active overbank deposition (Fig. 9). Proxy data reveal an interesting, partly coordinated pattern of vegetation variability through time (Fig. 9). Low tree density (a low D/P phytolith index) is generally associated with a lower aridity index (Iph phytolith index) and a biomarker signal of increased C_4 vegetation, which is likely humid-adapted grass or sedges based on the phytolith index (Iph). Plant wax $\delta^{13}C$ values broadly track the D/P index (Fig. 9). The highest Iph index (indicating more arid-adapted grasses) coincides with the greatest amount of woody cover, indicated by both D/P index and plant wax $\delta^{13}C$ values (Fig. 9; NL129-17:16.5 m). Notably, samples collected from the alternating paleosol and bedded silt sequence between NL129-17 13.5–16.6 m show the greatest shifts in vegetation dominance (Fig. 9). At 14.8 m, phytolith indices indicate higher proportions of humid grasses (low Iph) and less woody cover (low D/P) associated with a silty layer interpreted as a crevasse splay. At 15.9 m, within the overlying paleosol layer, there is a shift back to woody dicots based on phytolith D/P index and the $\delta^{13}C$ value of pedogenic carbonate (−7.9‰), suggesting a woodland or shrubland. The most dramatic shift in phytolith indices occurs between 15.9 and 16.6 m, when the grass community includes more humid-adapted Panicoideae grasses and has low tree density but then switches to arid-adapted grasses and more woody vegetation (Fig. 9). Patterns of high woody cover combined with arid-adapted grasses could result from local changes in the depositional environment but also suggest a larger-scale environmental driver such as changes in rainfall amount, regional temperature, and seasonality, which, in turn, affect evapotranspiration. Lower rainfall has been linked to higher tree density and greater amounts of C_4 grasses in modern Laetoli (Andrews and Bamford, 2008; Andrews et al., 2011). On orbital timescales, rainfall patterns vary in the Turkana Basin and thus could be a driver of the observed vegetation shifts (Feakins et al., 2007; Lupien et al., 2018, 2020).

Stable carbon isotopes from pedogenic carbonates in the NL129-17 section indicate C_3 woody to mixed C_3–C_4 vegetation through time but do not offer similar resolution for the major shifts in vegetation recorded by phytoliths and plant biomarkers (Fig. 9). This may be because some of the pedogenic carbonates were recovered from different layers within the NL129-17 section than the plant waxes or phytoliths (Fig. 9). However, it could also result from greater time averaging in each individual pedogenic carbonate specimen as compared to the signal preserved in the phytolith assemblages and biomarker proxies. Alternatively, pedogenic carbonates could be biased toward carbonate precipitation during times when more C_3 plants are affecting soil chemistry through increased transpiration, such as dry seasons (e.g., Meyer et al., 2014; Huth et al., 2019).

Examining proxy associations with the different lithofacies in more detail, the tree density index (D/P) suggests increased woody cover associated with three of the well-developed paleosols in NL129-17, including the paleosol immediately above the hominin site. Lower woody cover, combined with higher humid grasses based on the Iph index, coincides with some bedded sedimentary layers, indicating intervals of rapid floodplain aggradation. Each of the paleosols likely represents 10^2–10^3 years or longer, given their well-developed pedogenic features, including dish structures and carbonate nodules. These nodules form over tens to thousands of years (Zamanian et al., 2016). The six distinct fining upward cycles between 4.5 and 16 m on NL129-17 could represent 10^3–10^4 years each, for an estimated total time span of 6000–60,000 years, which is within the range of documented semiarid floodplain sedimentary rates (Daniels, 2003). This means a rate of overall sediment accumulation between ~2 and 20 cm/1000 yrs, with the latter being more in line with other calculations for the Koobi Fora Formation (Campisano and Feibel, 2007). The bounding dates (3.596–3.44 Ma) for the NL129-17 section give a maximum time span of ~150 kyr. It is thus reasonable to estimate that fine-grained lithofacies between the sand bodies represent tens of thousands of years within this interval, long enough to be affected by Milankovitch or other shorter-term climate cycles.

The sample sizes associated with this section are too small to test for correlations between depositional facies and vegetation type. However, proxies derived from paleosols generally preserve higher levels of C_3 vegetation and are often associated with greater

proportions of arid-adapted grasses (Iph index). Phytoliths collected from silty sediments associated with floodplain or crevasse splays have a lower D/P index compared to those collected from well-developed paleosols, but plant wax biomarkers do not always show the same strong pattern of greater C_4 biomass in silty sediments. Pedogenic carbonates have a relatively limited $\delta^{13}C$ range, from −6.0‰ to nearly −8.7‰, indicating low levels of C_4 biomass (average = 20%) throughout the section. In contrast, plant wax $\delta^{13}C$ shows a much higher variability (~10‰ range) and indicates higher abundance of C_4 biomass (average = 49%) for the sampled intervals of the NL129-17 section. The offset between pedogenic and plant wax carbon isotopes has also been observed in other parts of the Turkana Basin and is discussed in detail, but not resolved, in Uno et al. (2016).

4.3. Local and regional comparisons of contemporaneous proxies provide insight into their biases

The vegetation proxies (pedogenic carbonates, plant wax biomarkers, and phytoliths) from the geologic sections associated with ET03-166/168 each represent relatively small spatial scales (local) and provide variably time-averaged information. The fact that phytoliths and plant wax biomarkers show strong shifts from grass to woody-dominated ecosystems through time indicates that temporal and spatial averaging in these samples is less than the temporal and spatial scale of environmental change between the sample levels. Pedogenic carbonate $\delta^{13}C$ signals, however, consistently represent high levels of C_3 woody cover (forest to woodland/shrubland) through the same sample interval. The differences in signal could be due to the greater time averaging of pedogenic carbonate nodules, which averages short-term vegetation change. Phytoliths and biomarkers, in contrast, may have high turnover rates in biologically and chemically active substrates and are therefore weighted toward sampling a short period of time prior to final burial. Furthermore, phytoliths and plant wax biomarkers can be deposited and preserved in a greater range of sedimentary environments than pedogenic carbonates, which are generally restricted to soils that experience strong rainfall seasonality and mean annual rainfall of ~400–1000 mm and therefore form only seasonally and in specific conditions (Breecker et al., 2009; Meyer et al., 2014). Thus, differences among the vegetation proxies used in this study affect paleoenvironmental interpretations, and their offsets are an intriguing result of our study that should be investigated further.

Within the broader Area 129 temporospatial region (Fig. 1), $\delta^{13}C$ values from large herbivore enamel represent more C_4 vegetation on average than do those from the pedogenic carbonates (Fig. 10). This supports the hypothesis that mammal enamel from fossil herbivore communities represents larger spatial scales, and thus greater spatial averaging of vegetation, than other vegetation proxies (Du et al., 2019). Biases toward C_4 consumption in enamel could also be influenced by observations of high abundances of grazers across multiple habitat types, including those with high levels of woody cover (Negash and Barr, 2023). However, Du et al. (2019) reported that $\delta^{13}C$ values of pedogenic carbonates represent more C_3 environments across the Plio-Pleistocene Afar and Turkana Basins compared to $\delta^{13}C$ values from mammalian tooth enamel. Uno et al. (2016) find that plant wax biomarkers indicate 25–30% more C_4 biomass on the landscape than do coeval pedogenic carbonates in the Pleistocene terrestrial sediments of West Turkana. Our data from Area 129 further support these observations of biases among proxies (Fig. 10), particularly that pedogenic carbonates are biased toward a C_3 signal compared to other vegetation proxies.

4.4. Interbasin comparisons suggest aridity characterizes the Pliocene eastern African basin

The new hominin specimens from Area 129 support the hypothesis that hominins were widespread but rare compared to other large fauna in the middle Pliocene Turkana Basin (Bobe et al., 2002; Su and Harrison, 2008; Villaseñor et al., 2020). At East Turkana, they represent slightly more than 1% of the fossil large mammal specimens, which is consistent with previous observations of hominin abundances from this region (Villaseñor et al., 2020). West Turkana shows a higher relative abundance of hominins than East Turkana, but with low sample sizes overall. Previous research suggests that the high numbers of hominin specimens and low samples of other rare fauna are due to sampling and reporting biases (Villaseñor et al., 2020). East Turkana has the largest published faunal sample identified to tribe from the 3.59–3.44 Ma interval (n = 273 specimens) and the most even distribution of identified tribes compared to the three other contemporaneous sites in this study: Hadar/Dikika, the Lower Omo Valley, and West Turkana. The most abundant two tribes in East Turkana, Alcelaphini and Tragelaphini, are associated with open grasslands and mixed grassland-woodland environments in the Pliocene, respectively (Cerling et al., 2015; Fig. 8). Since bovids represent nearly 40% of specimens at East Turkana, these mammalian distributions support the reconstruction of a region with heterogeneous C_3/C_4 vegetation at regional scales (Cerling et al., 2015; Villaseñor et al., 2020). Paleoenvironmental data from ET03-166/168 suggest the mixed C_3/C_4 vegetation represents shifts between more arid C_3-dominated environments and wetter C_4-dominated environments.

Though published faunal collections from other middle Pliocene regions are limited in sample size, paleoenvironmental proxies such as pedogenic carbonates, plant wax biomarkers, and pollen records have a more robust spatiotemporal record. Liddy et al. (2016) found that $\delta^{13}C$ values from plant waxes from the Gulf of Aden suggest a high abundance of C_3 vegetation at the regional scale between 3.8 and 3.0 Ma, specifically arid-adapted C_3 taxa in Amaranthaceae, based on corresponding pollen data from the same core (DSDP 231). Grass pollen is very low in abundance during this period. Cerling et al. (2011) also found that the Turkana Basin experienced a period of increasing woody cover after 3.6 Ma, compared to the Late Miocene and Early Pliocene paleoenvironments, based on pedogenic carbonate $\delta^{13}C$ values. Lake Lokochot would have supported mesic environments near the lakeshore, particularly on the east side of present-day Lake Turkana, which represents the gently sloping hanging wall of a half-graben bounded by a major, basin-forming normal fault on its west side (Brown and Feibel, 1986). However, these mesic conditions could have waxed and waned with shifting depositional environments as well as climate cycles, leading to the local temporal changes in vegetation documented in this study (Fig. 9). To the north, the Afar basin also experienced a peak in woody cover during the middle Pliocene, but later than in the Turkana Basin (Cerling et al., 2011). Assuming pedogenic carbonates regularly form during periods of higher seasonality and water deficits (Cerling, 1984), the increase in C_3 vegetation indicated by pedogenic carbonates could support other records of Pliocene aridity from northeast Africa (Liddy et al., 2016).

These findings add ecological depth to the habitat reconstructions of other middle Pliocene hominin sites from nearby regions. For example, Harmand et al. (2015) suggest that the stone tools found on the opposite side of the Turkana basin two hundred thousand years later, at ~3.3 Ma, are associated with a woody or shrubby environment based on pedogenic carbonates and associated mammalian taxa. Leakey et al. (2001) make the same interpretation about environments using the faunal evidence, particularly the presence of *Theropithecus brumpti*, to suggest that

K. platyops specimens are associated with higher levels of woody cover. As noted in this study and several others (Uno et al., 2016; Du et al., 2019), pedogenic carbonates may be biased toward C_3 biomass compared to other proxies. Furthermore, the C_3 signal in the Turkana Basin could indicate arid-adapted woody taxa, suggesting that environments occupied by Pliocene hominins incorporated regions with prolonged water deficits (Blumenthal et al., 2017).

4.5. Biome reconstructions of the middle Pliocene aid in defining the hominin niche

The middle Pliocene Turkana Basin may represent a non-analogue ecosystem, i.e., a combination of climate and vegetation types that is not present on the modern tropical African landscapes. This region of the EARS has hosted topographically varied ecosystems for tens of millions of years; high temperatures and water deficits have likely been important ecological characteristics of the low-elevation rift landscapes for at least four million years, although annual rainfall was likely higher than today (Passey et al., 2010; Fortelius et al., 2016; Blumenthal et al., 2017). As represented in this study and other analyses through time, a mixed C_3 and C_4 ecosystem was an important component of the regional Pliocene biomes associated with hominins in the rift valley (Cerling et al., 2011; Levin et al., 2011; Paquette and Drapeau, 2021). Furthermore, since arid-adapted grasses and high proportions of C_3 biomass are associated in this study (Fig. 9), it is possible that the C_3 biomass included arid-adapted plant taxa, such as those characterizing the vegetation community of the Turkana region today. Additionally, local shifts in hydrology would have exerted important controls on vegetation composition through time that affected the habitability of hominin sites within semiarid regions (Cuthbert et al., 2017; Barboni et al., 2019; Joordens et al., 2019).

Both *A. afarensis* and *K. platyops* are known from the middle Pliocene Turkana Basin (Kimbel, 1988; Leakey et al., 2001). Between 3.6 and 3.0 Ma, the *A. afarensis* range spans from northern Ethiopia to Tanzania's lowland rift valley basins, indicating a large functional niche of *A. afarensis* (Bonnefille et al., 2004; Reed, 2008; Su and Harrison, 2015). In contrast, the documented spatiotemporal range of *K. platyops* is more restricted; the type and paratype specimens date to between 3.5 and 3.3Ma, and all specimens associated with this taxon derive from West Turkana, Kenya (Leakey et al., 2001; Skinner et al., 2020). Of course, it is possible that this species occurred in different regions of Africa that did not preserve fossils, such as central African biomes.

The multiproxy data in this study, particularly the vegetation proxies from ET03-168/166, demonstrate that middle Pliocene hominin fossils in the Turkana Basin were most closely associated with mesic grasses and mixed C_3–C_4 biomass within a region that likely included substantial arid-adapted C_3 biomass (Gibert et al., 2022). This adds to a growing body of literature indicating that, rather than being tied to C_3, tree-dominated habitats, the Pliocene hominin environmental niche (including the *Australopithecus anamensis* lineage) included mixed C_3 and C_4 vegetation (i.e., open, wooded grasslands and other types of mixed wooded-grassy vegetation, e.g., Bobe et al., 2020). This pattern is further supported by the fact that relatively few Pliocene hominins are found in sedimentary deposits that preserve evidence for extensive woodland vegetation, such as the Lower Omo Valley in Ethiopia (Bobe et al., 2002; Villaseñor et al., 2020) and Lothagam (Leakey and Harris, 2003). Thus, we suggest that Pliocene hominins utilized mesic habitats within regions characterized as semiarid and seasonally water-limited, such as those in the present-day Turkana basin. Utilizing mesic environments within semiarid biomes would have increased the ability of early hominins to move and inhabit a wide range of ecosystems by introducing new niche space and potential corridors within the basin of the rift valley that were not available to other species of Pliocene apes (Cuthbert et al., 2017; Joordens et al., 2019).

5. Conclusions

The new hominins from Area 129 and the associated vegetation proxies demonstrate not only that both C_3 and C_4 biomass were important components of Pliocene Turkana Basin ecology but that multiproxy comparisons give a more nuanced view of the region across scales. Though it is unclear how hominins utilized Pliocene biomes beyond consuming a mix of C_3 and C_4 plant types, this study shows that one geographically restricted part of the Turkana Basin offered local habitats ranging from C_4-dominated to C_3-dominated environments that fluctuated over relatively short time intervals ($\sim 10^4$ years or less). Periods when C_3 plants dominated were associated with greater levels of arid-adapted C_4 grasses. Combined with previous studies, this study supports the hypothesis that mesic environments within semiarid regions were an important facet of the hominin niche. Multiproxy evidence combined with detailed stratigraphy of the hominin site (ET03-166/168) allows a richer and more nuanced reconstruction of the environments than would any single proxy. Multiproxy isotopic evidence also supports the hypothesis that carbon isotopes from pedogenic carbonates are C_3 biased relative to plant wax biomarkers and enamel isotopes. A similar, spatially focused multiproxy approach in other regions that preserve proportionally more hominins than East Turkana, such as Hadar, Dikika, or Woranso-Mille in Ethiopia, and West Turkana in Kenya, would further define the range of rift valley habitats, provide boundaries for the Pliocene hominin niche, and further resolve the limitations of the most common environmental proxies.

Acknowledgments

We thank the many skilled Kenyan field workers and fossil collectors. This research would not be possible without them. We are grateful to the National Museums of Kenya, NACOSTI, the Koobi Fora Field School, and the many field school students who participated in data collection and processing. We acknowledge Naomi Levin and Christopher Campisano, whose careful geologic and paleoecological records were foundational to this paper. We are grateful to the three anonymous reviewers, the Associate Editor, and the JHE Editor, Andrea Taylor, whose questions and insights improved the manuscript. We also thank Lucas Delezene for carefully editing the manuscript many times. This research was funded by the Leakey Foundation, the National Science Foundation (SBE-1534824 and SBE-1624398), and the Ford Foundation. D.V.P. also acknowledges the Fundação de Amparo à Pesquisa do Estado de São Paulo (FAPESP) for financial support through grant 2018/20733-6.

Supplementary Online Material

Supplementary online material to this article can be found online at https://doi.org/10.1016/j.jhevol.2023.103385.

References

Albert, R.M., Bamford, M.K., 2012. Vegetation during UMBI and deposition of Tuff IF at Olduvai Gorge, Tanzania (ca. 1.8 Ma) based on phytoliths and plant remains. J. Hum. Evol. 63, 342–350.

Albert, R.M., Bamford, M.K., Cabanes, D., 2006. Taphonomy of phytoliths and macroplants in different soils from Olduvai Gorge (Tanzania) and the application to Plio-Pleistocene palaeoanthropological samples. Quat. Int. 148, 78–94.

Albert, R.M., Bamford, M.K., Cabanes, D., 2009. Palaeoecological significance of palms at Olduvai Gorge, Tanzania, based on phytolith remains. Quat. Int. 193, 41–48.

Albert, R.M., Weiner, S., 2001. Study of phytoliths in prehistoric ash layers from Kebara and Tabun caves using a quantitative approach. In: Meunier, J.D., Colin, F. (Eds.), Phytoliths: Applications in Earth Sciences and Human History. CRC Press, London, pp. 251–266.
Alemseged, Z., Bobe, R., Geraads, D., 2007. Comparability of fossil data and its significance for the interpretation of hominin environments. In: Bobe, R., Alemseged, Z., Behrensmeyer, A.K. (Eds.), Hominin Environments in the East African Pliocene: An Assessment of the Faunal Evidence. Springer Netherlands, Dordrecht, pp. 159–181.
Alexandré, A., Meunier, J.-D., Lézine, A.-M., Vincens, A., Schwartz, D., 1997. Phytoliths: Indicators of grassland dynamics during the late Holocene in intertropical Africa. Palaeogeogr. Palaeoclimatol. Palaeoecol. 136, 213–229.
Andrews, P., Bamford, M., 2008. Past and present vegetation ecology of Laetoli, Tanzania. J. Hum. Evol. 54, 78–98.
Andrews, P., Bamford, M.K., Njau, E.-F., Leliyo, G., 2011. The ecology and biogeography of the Endulen-Laetoli area in northern Tanzania. In: Paleontology and Geology of Laetoli: Human Evolution in Context. Springer, Dordrecht, pp. 167–200.
Ashley, G.M., Tactikos, J.C., Owen, R.B., 2009. Hominin use of springs and wetlands: Paleoclimate and archaeological records from Olduvai Gorge (~ 1.79–1.74 Ma). Palaeogeogr. Palaeoclimatol. Palaeoecol. 272, 1–16.
Barboni, D., Ashley, G.M., Bourel, B., Arraiz, H., Mazur, J.-C., 2019. Springs, palm groves, and the record of early hominins in Africa. Rev. Palaeobot. Palynol. 266, 23–41.
Barboni, D., Ashley, G.M., Dominguez-Rodrigo, M., Bunn, H.T., Mabulla, A.Z.P., Baquedano, E., 2010. Phytoliths infer locally dense and heterogeneous paleovegetation at FLK North and surrounding localities during upper Bed I time, Olduvai Gorge, Tanzania. Quat. Res. 74, 344–354.
Barr, W.A., 2015. Paleoenvironments of the Shungura Formation (Plio-Pleistocene: Ethiopia) based on ecomorphology of the bovid astragalus. J. Hum. Evol. 88, 97–107.
Bedaso, Z.K., Wynn, J.G., Alemseged, Z., Geraads, D., 2013. Dietary and paleoenvironmental reconstruction using stable isotopes of herbivore tooth enamel from middle Pliocene Dikika, Ethiopia: Implication for *Australopithecus afarensis* habitat and food resources. J. Hum. Evol. 64, 21–38.
Behrensmeyer, A.K., 1988. Vertebrate preservation in fluvial channels. Palaeogeogr. Palaeoclimatol. Palaeoecol. 63, 183–199.
Behrensmeyer, A.K., Barry, J., 2005. Biostratigraphic surveys in the Siwaliks of Pakistan: A method for standardized surface sampling of the vertebrate fossil record. Palaeontol. Electron. 8, 1–24.
Behrensmeyer, A.K., Kidwell, S.M., 1985. Taphonomy's contributions to paleobiology. Paleobiology 11, 105–119.
Behrensmeyer, A.K., Kidwell, S.M., Gastaldo, R.A., 2000. Taphonomy and paleobiology. Paleobiology 26, 103–147.
Behrensmeyer, A.K., Reed, K.E., 2013. Reconstructing the habitats of *Australopithecus*: Paleoenvironments, site taphonomy, and faunas. In: Reed, K.E., Fleagle, J.G., Leakey, R.E. (Eds.), The Paleobiology of *Australopithecus*. Springer, Amsterdam, pp. 41–60.
Behrensmeyer, A.K., Quade, J., Cerling, T.E., Kappelman, J., Khan, I.A., Copeland, P., Roe, L., Hicks, J., Stubblefield, P., Willis, B.J., 2007. The structure and rate of late Miocene expansion of C4 plants: Evidence from lateral variation in stable isotopes in paleosols of the Siwalik Group, northern Pakistan. Geol. Soc. Am. Bull. 119, 1486–1505.
Blumenthal, S.A., Levin, N.E., Brown, F.H., Brugal, J.-P., Chritz, K.L., Harris, J.M., Jehle, G.E., Cerling, T.E., 2017. Aridity and hominin environments. Proc. Natl. Acad. Sci. USA 114, 7331–7336.
Bobe, R., 2006. The evolution of arid ecosystems in eastern Africa. J. Arid Environ. 66, 564–584.
Bobe, R., 2011. Fossil mammals and paleoenvironments in the Omo-Turkana Basin. Evol. Anthropol. 20, 254–263.
Bobe, R., Behrensmeyer, A.K., Chapman, R.E., 2002. Faunal change, environmental variability and late Pliocene hominin evolution. J. Hum. Evol. 42, 475–497.
Bobe, R., Behrensmeyer, A.K., Eck, G.G., Harris, J.M., 2007. Patterns of abundance and diversity in late Cenozoic bovids from the Turkana and Hadar Basins, Kenya and Ethiopia. In: Bobe, R., Alemseged, Z., Behrensmeyer, A.K. (Eds.), Hominin Environments in the East African Pliocene: An Assessment of the Faunal Evidence. Springer Netherlands, Dordrecht, pp. 129–157.
Bobe, R., Eck, G.G., 2001. Responses of African bovids to Pliocene climatic change. Paleobiology 27, 1–47.
Bobe, R., Manthi, F.K., Ward, C.V., Plavcan, J.M., Carvalho, S., 2020. The ecology of *Australopithecus anamensis* in the early Pliocene of Kanapoi, Kenya. J. Hum. Evol. 140, 102717.
Bonnefille, R., 2010. Cenozoic vegetation, climate changes and hominid evolution in tropical Africa. Glob. Planet. Change 72, 390–411.
Bonnefille, R., Potts, R., Chalié, F., Jolly, D., Peyron, O., 2004. High-resolution vegetation and climate change associated with Pliocene *Australopithecus afarensis*. Proc. Natl. Acad. Sci. USA 101, 12125–12129.
Breecker, D.O., Sharp, Z.D., McFadden, L.D., 2009. Seasonal bias in the formation and stable isotopic composition of pedogenic carbonate in modern soils from central New Mexico, USA. Geol. Soc. Am. Bull. 121, 630–640.
Bremond, L., Alexandre, A., Hély, C., Guiot, J., 2005. A phytolith index as a proxy of tree cover density in tropical areas: Calibration with Leaf Area Index along a forest–savanna transect in southeastern Cameroon. Glob. Planet. Change 45, 277–293.
Bremond, L., Alexandre, A., Wooller, M.J., Hély, C., Williamson, D., Schäfer, P.A., Majule, A., Guiot, J., 2008a. Phytolith indices as proxies of grass subfamilies on East African tropical mountains. Glob. Planet. Change 61, 209–224.
Bremond, L., Alexandre, A., Peyron, O., Guiot, J., 2008b. Definition of grassland biomes from phytoliths in West Africa. J. Biogeogr. 35, 2039–2048.
Brown, F.H., 1982. Tulu Bor tuff at Koobi Fora correlated with the Sidi Hakoma tuff at Hadar. Nature 300, 631–633.
Brown, F.H., Feibel, C.S., 1986. Revision of lithostratigraphic nomenclature in the Koobi Fora region, Kenya. J. Geol. Soc. 143, 297–310.
Brown, F.H., Feibel, C.S., 1991. Stratigraphy, depositional environments and palaeogeography of the Koobi Fora Formation. Koobi Fora Research Project 3, 1–30.
Brown, F.H., Mcdougall, I., 2011. Geochronology of the Turkana Depression of Northern Kenya and Southern Ethiopia. Evol. Anthropol. 20, 217–227.
Bruhn, R.L., Brown, F.H., Gathogo, P.N., Haileab, B., 2011. Pliocene volcano-tectonics and paleogeography of the Turkana Basin, Kenya and Ethiopia. J. Afr. Earth Sci. 59, 295–312.
Campisano, C.J., Feibel, C.S., 2007. Connecting local environmental sequences to global climate patterns: Evidence from the hominin-bearing Hadar Formation, Ethiopia. J. Hum. Evol. 53, 515–527.
Campisano, C.J., Feibel, C.S., 2008. Depositional environments and stratigraphic summary of the Pliocene Hadar formation at Hadar, Afar depression, Ethiopia. In: Quade, J., Wynn, J.G. (Eds.), The Geology of Early Humans in the Horn of Africa, Geological Society of America Special Paper 446, pp. 179–201.
Cerling, T.E., 1984. The stable isotopic composition of modern soil carbonate and its relationship to climate. Earth Planet. Sci. Lett. 71, 229–240.
Cerling, T.E., Andanje, S.A., Blumenthal, S.A., Brown, F.H., Chritz, K.L., Harris, J.M., Hart, J.A., Kirera, F.M., Kaleme, P., Leakey, L.N., 2015. Dietary changes of large herbivores in the Turkana Basin, Kenya from 4 to 1 Ma. Proc. Natl. Acad. Sci. USA 112, 11467–11472.
Cerling, T.E., Brown, F.H., 1982. Tuffaceous marker horizons in the Koobi Fora region and the Lower Omo Valley. Nature 299, 216–221.
Cerling, T.E., Harris, J.M., 1999. Carbon isotope fractionation between diet and bioapatite in ungulate mammals and implications for ecological and paleoecological studies. Oecologia 120, 347–363.
Cerling, T.E., Harris, J.M., MacFadden, B.J., Leakey, M.G., Quade, J., Eisenmann, V., Ehieringer, J.R., 1997. Global vegetation change through the Miocene/Pliocene boundary. Nature 389, 153–158.
Cerling, T., Quade, J., 1993. Stable carbon and oxygen isotopes in soil carbonates. In: Swart, P., McKenzie, J., Lohman, K. (Eds.), Continental Indicators of Climate. Geophysical Union Monograph, Jackson Hole, pp. 217–231.
Cerling, T.E., Wynn, J.G., Andanje, S.A., Bird, M.I., Korir, D.K., Levin, N.E., MacE, W., MacHaria, A.N., Quade, J., Remien, C.H., 2011. Woody cover and hominin environments in the past 6-million years. Nature 476, 51–56.
Cerling, T.E., Manthi, F.K., Mbua, E.N., Leakey, L.N., Leakey, M.G., Leakey, R.E., Brown, F.H., Grine, F.E., Hart, J.A., Kaleme, P., 2013. Stable isotope-based diet reconstructions of Turkana Basin hominins. Proc. Natl. Acad. Sci. USA 110, 10501–10506.
Chikaraishi, Y., Naraoka, H., 2001. Organic hydrogen-carbon isotope signatures of terrestrial higher plants during biosynthesis for distinctive photosynthetic pathways. Geochem. J. 35, 451–458.
Chikaraishi, Y., Naraoka, H., 2003. Compound-specific δD–δ13C analyses of *n*-alkanes extracted from terrestrial and aquatic plants. Phytochemistry 63, 361–371.
Curran, S.C., Haile-Selassie, Y., 2016. Paleoecological reconstruction of hominin-bearing middle Pliocene localities at Woranso-Mille, Ethiopia. J. Hum. Evol. 96, 97–112.
Cuthbert, M.O., Gleeson, T., Reynolds, S.C., Bennett, M.R., Newton, A.C., McCormack, C.J., Ashley, G.M., 2017. Modelling the role of groundwater hydrorefugia in East African hominin evolution and dispersal. Nat. Commun. 8, 15696.
Daniels, J.M., 2003. Floodplain aggradation and pedogenesis in a semiarid environment. Geomorphology 56, 225–242.
Davis, M., Pineda-Munoz, S., 2016. The temporal scale of diet and dietary proxies. Ecol. Evol. 6, 1883–1897.
Delezene, L.K., Zolnierz, M.S., Teaford, M.F., Kimbel, W.H., Grine, F.E., Ungar, P.S., 2013. Premolar microwear and tooth use in *Australopithecus afarensis*. J. Hum. Evol. 65, 282–293.
Drapeau, M.S.M., Ward, C.V., Kimbel, W.H., Johanson, D.C., Rak, Y., 2005. Associated cranial and forelimb remains attributed to *Australopithecus afarensis* from Hadar, Ethiopia. J. Hum. Evol. 48, 593–642.
Du, A., Alemseged, Z., 2018. Diversity analysis of Plio-Pleistocene large mammal communities in the Omo-Turkana Basin, eastern Africa. J. Hum. Evol. 124, 25–39.
Du, A., Robinson, J.R., Rowan, J., Lazagabaster, I.A., Behrensmeyer, A.K., 2019. Stable carbon isotopes from paleosol carbonate and herbivore enamel document differing paleovegetation signals in the eastern African Plio-Pleistocene. Rev. Palaeobot. Palynol. 261, 41–52.
Eck, G.G., 2007. The effects of collection strategy and effort on faunal recovery. In: Bobe, R., Alemseged, Z., Behrensmeyer, A.K. (Eds.), Hominin Environments in the East African Pliocene: An Assessment of the Faunal Evidence. Springer Netherlands, Dordrecht, pp. 183–215.
Efron, B., Tibshirani, R.J., 1994. An Introduction to the Bootstrap. Chapman and Hall CRC Press, Boca Raton.
Eglinton, G., Hamilton, R.J., 1967. Leaf Epicuticular Waxes: The waxy outer surfaces of most plants display a wide diversity of fine structure and chemical constituents. Science 156, 1322–1335.

Feakins, S.J., Eglinton, T.I., demenocal, P.B., 2007. A comparison of biomarker records of northeast African vegetation from lacustrine and marine sediments (ca. 3.40 Ma). Org. Geochem. 38, 1607–1624.
Feibel, C.S., 2011. A geological history of the Turkana Basin. Evol. Anthropol. 20, 206–216.
Fernández-Jalvo, Y., Andrews, P., 2016. Atlas of Taphonomic Identifications: 1001+ Images of Fossil and Recent Mammal Bone Modification. Springer, Dordrechet.
Fernández-Jalvo, Y., Andrews, P., Denys, C., Sesé, C., Stoetzel, E., Marin-Monfort, D., Pesquero, D., 2016. Taphonomy for taxonomists: Implications of predation in small mammal studies. Quat. Sci. Rev. 139, 138–157.
Fortelius, M., Žliobaitė, I., Kaya, F., Bibi, F., Bobe, R., Leakey, L., Leakey, M., Patterson, D., Rannikko, J., Werdelin, L., 2016. An ecometric analysis of the fossil mammal record of the Turkana Basin. Philos. Trans. R. Soc. B Biol. Sci. 371, 20150232.
Francey, R.J., Allison, C.E., Etheridge, D.M., Trudinger, C.M., Enting, I.G., Leuenberger, M., Langenfelds, R.L., Michel, E., Steele, L.P., 1999. A 1000-year high precision record of δ13C in atmospheric CO2. Tellus B 51, 170–193.
Frost, S.R., Ward, C.V., Manthi, F.K., Plavcan, J.M., 2020. Cercopithecid fossils from Kanapoi, West Turkana, Kenya (2007–2015). J. Hum. Evol. 140, 102642.
Garcin, Y., Schefuß, E., Schwab, V.F., Garreta, V., Gleixner, G., Vincens, A., Todou, G., Séné, O., Onana, J.-M., Achoundong, G., 2014. Reconstructing C3 and C4 vegetation cover using *n*-alkane carbon isotope ratios in recent lake sediments from Cameroon, Western Central Africa. Geochim. Cosmochim. Acta 142, 482–500.
Gibert, C., Vignoles, A., Contoux, C., Banks, W.E., Barboni, D., Boisserie, J.-R., Chavasseau, O., Fluteau, F., Guy, F., Noûs, C., 2022. Climate-inferred distribution estimates of mid-to-late Pliocene hominins. Glob. Planet. Change 210, 103756.
Haile-Selassie, Y., Gibert, L., Melillo, S.M., Ryan, T.M., Alene, M., Deino, A., Saylor, B.Z., 2015. New species from Ethiopia further expands Middle Pliocene hominin diversity. Nature 521, 483–488.
Harmand, S., Lewis, J.E., Feibel, C.S., Lepre, C.J., Prat, S., Lenoble, A., Boës, X., Quinn, R.L., Brenet, M., Arroyo, A., 2015. 3.3-million-year-old stone tools from Lomekwi 3, West Turkana, Kenya. Nature 521, 310–315.
Harris, J.M., Brown, F.H., Leakey, M.G., Walker, A.C., Leakey, R.E., 1988. Pliocene and Pleistocene hominid-bearing sites from west of Lake Turkana, Kenya. Science 239, 27–33.
Harrison, T. (Ed.), 2011a. Paleontology and Geology of Laetoli: Human Evolution in Context. Geology, Geochronology, Paleoecology and Paleoenvironment, vol. 1. Springer, Dordrecht.
Harrison, T. (Ed.), 2011b. Paleontology and Geology of Laetoli: Human Evolution in Context. Fossil Hominins and the Associated Fauna, vol. 2. Springer, Dordrecht.
Hillhouse, J.W., Ndombi, J.W.M., Cox, A., Brock, A., 1977. Additional results on palaeomagnetic stratigraphy of the Koobi Fora Formation, east of Lake Turkana (Lake Rudolf), Kenya. Nature 265, 411–415.
Huth, T.E., Cerling, T.E., Marchetti, D.W., Bowling, D.R., Ellwein, A.L., Passey, B.H., 2019. Seasonal bias in soil carbonate formation and its implications for interpreting high-resolution paleoarchives: Evidence from southern Utah. J. Geophys. Res. Biogeosci. 124, 616–632.
Joordens, J.C.A., Feibel, C.S., Vonhof, H.B., Schulp, A.S., Kroon, D., 2019. Relevance of the eastern African coastal forest for early hominin biogeography. J. Hum. Evol. 131, 176–202.
Kimbel, W.H., 1988. Identification of a partial cranium of *Australopithecus afarensis* from the Koobi Fora Formation, Kenya. J. Hum. Evol. 17, 647–656.
Kimbel, W.H., Delezene, L.K., 2009. Lucy" redux: A review of research on *Australopithecus afarensis*. Am. J. Phys. Anthropol. 140, 2–48.
Kimbel, W.H., Johanson, D.C., Rak, Y., 1994. The first skull and other new discoveries of *Australopithecus afarensis* at Hadar, Ethiopia. Nature 368, 449–451.
Leakey, M.G., Harris, J.M., 2003. Lothagam: The Dawn of Humanity in Eastern Africa. Columbia University Press, New York.
Leakey, M.G., Spoor, F., Brown, F.H., Gathogo, P.N., Kiarie, C., Leakey, L.N., McDougall, I., 2001. New hominin genus from eastern Africa shows diverse middle Pliocene lineages. Nature 410, 433–440.
Leakey, R.E.F., 1976. New hominid fossils from the Koobi Fora formation in northern Kenya. Nature 261, 574–576.
Lee-Thorp, J.A., Sponheimer, M., Luyt, J., 2007. Tracking changing environments using stable carbon isotopes in fossil tooth enamel: An example from the South African hominin sites. J. Hum. Evol. 53, 595–601.
Levin, N.E., 2013. Compilation of East Africa soil carbonate stable isotope data. https://doi.org/10.1594/IEDA/100231. Version 1.0.
Levin, N.E., Brown, F.H., Behrensmeyer, A.K., Bobe, R., Cerling, T.E., 2011. Paleosol carbonates from the Omo Group: Isotopic records of local and regional environmental change in East Africa. Palaeogeogr. Palaeoclimatol. Palaeoecol. 307, 75–89.
Levin, N.E., Haile-Selassie, Y., Frost, S.R., Saylor, B.Z., 2015. Dietary change among hominins and cercopithecids in Ethiopia during the early Pliocene. Proc. Natl. Acad. Sci. USA 112, 12304–12309.
Liddy, H.M., Feakins, S.J., Tierney, J.E., 2016. Cooling and drying in northeast Africa across the Pliocene. Earth Planet. Sci. Lett. 449, 430–438.
Lupien, R.L., Russell, J.M., Feibel, C., Beck, C., Castañeda, I., Deino, A., Cohen, A.S., 2018. A leaf wax biomarker record of early Pleistocene hydroclimate from West Turkana, Kenya. Quat. Sci. Rev. 186, 225–235.
Lupien, R.L., Russell, J.M., Grove, M., Beck, C.C., Feibel, C.S., Cohen, A.S., 2020. Abrupt climate change and its influences on hominin evolution during the early Pleistocene in the Turkana Basin, Kenya. Quat. Sci. Rev. 245, 106531.
Lupien, R.L., Russell, J.M., Subramanian, A., Kinyanjui, R., Beverly, E.J., Uno, K.T., de Menocal, P., Dommain, R., Potts, R., 2021. Eastern African environmental variation and its role in the evolution and cultural change of *Homo* over the last 1 million years. J. Hum. Evol. 157, 103028.
Manly, B.F., 2007. Randomization, Bootstrap and Monte Carlo Methods in Biology, 3rd ed. CRC Press, Boca Raton.
Manthi, F.K., Cerling, T.E., Chritz, K.L., Blumenthal, S.A., 2020. Diets of mammalian fossil fauna from Kanapoi, northwestern Kenya. J. Hum. Evol. 140, 102338.
Mbua, E., Kusaka, S., Kunimatsu, Y., Geraads, D., Sawada, Y., Brown, F.H., Sakai, T., Boisserie, J.-R., Saneyoshi, M., Omuombo, C., 2016. Kantis: A new *Australopithecus* site on the shoulders of the Rift Valley near Nairobi, Kenya. J. Hum. Evol. 94, 28–44.
Melillo, S.M., Gibert, L., Saylor, B.Z., Deino, A., Alene, M., Ryan, T.M., Haile-Selassie, Y., 2021. New Pliocene hominin remains from the Leado Dido'a area of Woranso-Mille, Ethiopia. J. Hum. Evol. 153, 102956.
Meyer, N.A., Breecker, D.O., Young, M.H., Litvak, M.E., 2014. Simulating the effect of vegetation in formation of pedogenic carbonate. Soil Sci. Soc. Am. J. 78, 914–924.
Monger, H.C., Cole, D.R., Buck, B.J., Gallegos, R.A., 2009. Scale and the isotopic record of C4 plants in pedogenic carbonate: From the biome to the rhizosphere. Ecology 90, 1498–1511.
Negash, E.W., Alemseged, Z., Bobe, R., Grine, F., Sponheimer, M., Wynn, J.G., 2020. Dietary trends in herbivores from the Shungura Formation, southwestern Ethiopia. Proc. Natl. Acad. Sci. USA 117, 21921–21927.
Negash, E.W., Barr, W.A., 2023. Relative abundance of grazing and browsing herbivores is not a direct reflection of vegetation structure: Implications for hominin paleoenvironmental reconstruction. J. Hum. Evol. 177, 103328.
O'Leary, M.H., 1981. Carbon isotope fractionation in plants. Phytochemistry 20, 553–567.
Paquette, J., Drapeau, M.S.M., 2021. Environmental comparisons of the Awash Valley, Turkana Basin and lower Omo Valley from upper Miocene to Holocene as assessed from stable carbon and oxygen isotopes of mammalian enamel. Palaeogeogr. Palaeoclimatol. Palaeoecol. 562, 110099.
Passey, B.H., Levin, N.E., Cerling, T.E., Brown, F.H., Eiler, J.M., 2010. High-temperature environments of human evolution in East Africa based on bond ordering in paleosol carbonates. Proc. Natl. Acad. Sci. USA 107, 11245–11249.
Peterson, P.M., Romaschenko, K., Johnson, G., 2010. A classification of the Chloridoideae (Poaceae) based on multi-gene phylogenetic trees. Mol. Phylogen. Evol. 55, 580–598.
Piperno, D.R., 2006. Phytoliths: A Comprehensive Guide for Archaeologists and Paleoecologists. Altamira Press, San Diego.
Polissar, P.J., D'Andrea, W.J., 2014. Uncertainty in paleohydrologic reconstructions from molecular δD values. Geochim. Cosmochim. Acta 129, 146–156.
Polissar, P.J., Uno, K.T., Phelps, S.R., Karp, A.T., Freeman, K.H., Pensky, J.L., 2021. Hydrologic changes drove the Late Miocene Expansion of C4 Grasslands on the Northern Indian Subcontinent. Paleoceanogr. Paleoclimatol. 36, e2020PA004108.
Potts, R., Behrensmeyer, A.K., Faith, J.T., Tryon, C.A., Brooks, A.S., Yellen, J.E., Deino, A.L., Kinyanjui, R., Clark, J.B., Haradon, C.M., 2018. Environmental dynamics during the onset of the Middle Stone Age in eastern Africa. Science 360, 86–90.
R Core Team, 2021. R: A language and environment for statistical computing. R Foundation for Statistical Computing, Vienna.
Raffi, I., Wade, B.S., Pälike, H., Beu, A.G., Cooper, R., Crundwell, M.P., Krijgsman, W., Moore, T., Raine, I., Sardella, R., 2020. The Neogene period. In: Gradstein, F.M., Ogg, J.G., Schmitz, M.D., Ogg, G.M. (Eds.), Geologic Time Scale 2020. Elsevier, Amsterdam, pp. 1141–1215.
Reed, K.E., 2008. Paleoecological patterns at the Hadar hominin site, Afar regional state, Ethiopia. J. Hum. Evol. 54, 743–768.
Reed, K.E., Campisano, C.J., 2012. The Hadar Geoinformatics Database. https://paleocore.org/projects/hrp/.
Ségalen, L., Lee-Thorp, J.A., Cerling, T., 2007. Timing of C4 grass expansion across sub-Saharan Africa. J. Hum. Evol. 53, 549–559.
Skinner, M.M., Leakey, M.G., Leakey, L.N., Manthi, F.K., Spoor, F., 2020. Hominin dental remains from the Pliocene localities at Lomekwi, Kenya (1982–2009). J. Hum. Evol. 145, 102820.
Smith, D.G., Putnam, P.E., 1980. Anastomosed river deposits: Modern and ancient examples in Alberta, Canada. Can. J. Earth Sci. 17, 1396–1406.
Spoor, F., Leakey, M.G., O'Higgins, P., 2016. Middle Pliocene hominin diversity: *Australopithecus deyiremeda* and *Kenyanthropus platyops*. Philos. Trans. R. Soc. B Biol. Sci. 371, 20150231.
Strömberg, C.A.E., 2003. The origin and spread of grass-dominated ecosystems during the Tertiary of North America and how it relates to the evolution of hypsodonty in equids. Ph.D. Dissertation, University of California, Berkeley.
Strömberg, C.A.E., 2009. Methodological concerns for analysis of phytolith assemblages: Does count size matter? Quat. Int. 193, 124–140.
Strömberg, C.A.E., Dunn, R.E., Madden, R.H., Kohn, M.J., Carlini, A.A., 2013. Decoupling the spread of grasslands from the evolution of grazer-type herbivores in South America. Nat. Commun. 4, 1478.
Strömberg, C.A.E., di Stilio, V.S., Song, Z., 2016. Functions of phytoliths in vascular plants: An evolutionary perspective. Funct. Ecol. 30, 1286–1297.
Strömberg, C.A.E., Dunn, R.E., Crifò, C., Harris, E.B., 2018. Phytoliths in paleoecology: Analytical considerations, current use, and future directions. In: Croft, D.A., Su, D.F., Simpson, S.W. (Eds.), Methods in Paleoecology: Reconstructing Cenozoic Terrestrial Environments and Ecological Communities. Springer, Cham, pp. 235–287.

Su, D.F., Haile-Selassie, Y., 2022. Mosaic habitats at Woranso-Mille (Ethiopia) during the Pliocene and implications for *Australopithecus* paleoecology and taxonomic diversity. J. Hum. Evol. 163, 103076.
Su, D.F., Harrison, T., 2008. Ecological implications of the relative rarity of fossil hominins at Laetoli. J. Hum. Evol. 55, 672–681.
Su, D.F., Harrison, T., 2015. The paleoecology of the Upper Laetolil Beds, Laetoli Tanzania: A review and synthesis. J. Afr. Earth Sci. 101, 405–419.
Tipple, B.J., Meyers, S.R., Pagani, M., 2010. Carbon isotope ratio of Cenozoic CO2: A comparative evaluation of available geochemical proxies. Paleoceanography 25, PA3202.
Twiss, P.C., 1992. Predicted world distribution of C 3 and C 4 grass phytoliths. In: Mulholland, S.C., Rapp, J.G. (Eds.), Phytolith Systematics. Plenum Press, New York, pp. 113–128.
Twiss, P.C., Suess, E., Smith, R.M., 1969. Morphological classification of grass phytoliths. Soil Sci. Soc. Am. J. 33, 109–115.
Ungar, P.S., Scott, R.S., Grine, F.E., Teaford, M.F., 2010. Molar microwear textures and the diets of *Australopithecus anamensis* and *Australopithecus afarensis*. Philos. Trans. R. Soc. B Biol. Sci. 365, 3345–3354.
Uno, K.T., Cerling, T.E., Harris, J.M., Kunimatsu, Y., Leakey, M.G., Nakatsukasa, M., Nakaya, H., 2011. Late Miocene to Pliocene carbon isotope record of differential diet change among East African herbivores. Proc. Natl. Acad. Sci. USA 108, 6509–6514.
Uno, K.T., Polissar, P.J., Kahle, E., Feibel, C., Harmand, S., Roche, H., Demenocal, P.B., 2016. A Pleistocene palaeovegetation record from plant wax biomarkers from the Nachukui Formation, West Turkana, Kenya. Philos. Trans. R. Soc. B Biol. Sci. 371, 20150235.
Villaseñor, A., Bobe, R., Behrensmeyer, A.K., 2020. Middle Pliocene hominin distribution patterns in Eastern Africa. J. Hum. Evol. 147, 102856.
Ward, C.V., Plavcan, J.M., Manthi, F.K., 2020. New fossils of *Australopithecus anamensis* from Kanapoi, West Turkana, Kenya (2012–2015). J. Hum. Evol. 140, 102368.
White, T.D., Suwa, G., Simpson, S., Asfaw, B., 2000. Jaws and teeth of *Australopithecus afarensis* from Maka, Middle Awash, Ethiopia. Am. J. Phys. Anthropol. 111, 45–68.
WoldeGabriel, G., Endale, T., White, T.D., Thouveny, N., Hart, W.K., Renne, P.R., Asfaw, B., 2013. The role of tephra studies in African paleoanthropology as exemplified by the Sidi Hakoma Tuff. J. Afr. Earth Sci. 77, 41–58.
Wynn, J.G., Alemseged, Z., Bobe, R., Grine, F.E., Negash, E.W., Sponheimer, M., 2020. Isotopic evidence for the timing of the dietary shift toward C4 foods in eastern African *Paranthropus*. Proc. Natl. Acad. Sci. USA 117, 21978–21984.
Zamanian, K., Pustovoytov, K., Kuzyakov, Y., 2016. Pedogenic carbonates: Forms and formation processes. Earth Sci. Rev. 157, 1–17.